JWST composite NIRCam-MIRI image of Stephan's Quintet (NASA/STScI)

Low Energy Ionizing Radiation and Plasma Contributions to Radiation Dose in Materials at Sun-Earth Lagrange Points

Joseph I. Minow, PhD
Technical Fellow for Space Environments
NASA Engineering and Safety Center
NASA, Marshall Space Flight Center

2023 Materials Research Society Spring Meeting
Symposium SF02: Materials in Space—Design and Testing
San Francisco, CA, 10-14 April 2023

joseph.minow@nasa.gov

Introduction

- High energy radiation environments responsible for radiation damage to thick materials are well characterized and modeled:
  - Galactic cosmic rays — Badhwar-O'Neil 2020, CREME96, Nymmik
  - Solar particle events — Emission of Solar Protons, SAPPHIRE, JPL, King 1972
  - Trapped radiation belts — AE8/AP8, AE9/AP9/IRENE

- Low energy radiation environments responsible for radiation damage to thin materials relevant to Lagrange points and interplanetary missions have not been treated as comprehensively to date:
  - Solar wind
  - Magnetosheath
  - Magnetotail

- Concern to spacecraft design and operations is radiation damage to surfaces and thin materials with mission critical applications on exterior of spacecraft
  - Applications: thermal control coatings, sunshields, multilayer insulation, optical thin film coatings, solar sails, thermo-optical properties of space exposed materials
  - Damage processes: radiation degradation (total dose), light ion sputtering, proton blistering of soft metals, modification of optical properties (α/ε), modification of charging properties (SEY, surface conductivity)

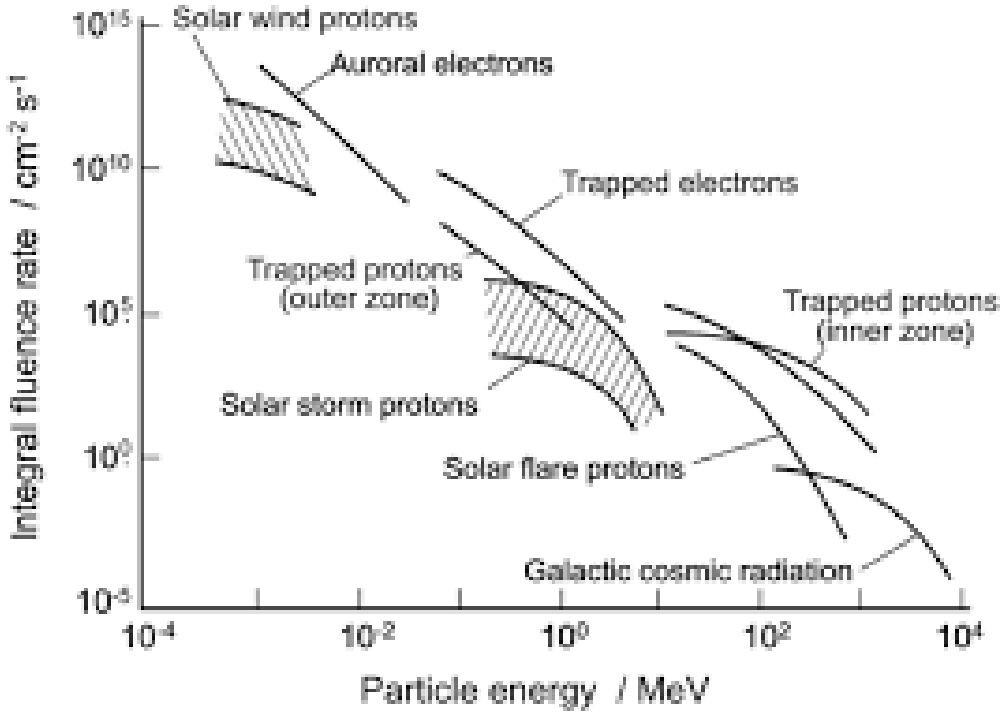

Sun-Earth Lagrange Points

- **Lagrange points** are the five locations in a three-body system where the gravitation forces of the two largest masses M1, M2 are balanced by the centripetal force required for the small object of mass M3 to move with no net relative motion with respect to M1, M2
  - Named after Joseph-Louis Lagrange (1736-1813) who discovered the points in his reformulated version of Newtonian mechanics
  - M1: Sun M2: Earth M3: satellite at Lagrange point

- **Stability**
  - L1, L2, L3 are unstable, a small displacement from the Lagrange points will continue to grow and the small mass will drift away.
  - L4,L5 are stable to small displacements.

- **Station-keeping** fuel requirements are minimal to maintain orbits about the unstable Lagrange points

- **L1, L2** are about 1.5×10^6 km from Earth (~235 Re from Earth or ~0.01 AU)

- **Lagrange points have a number of useful characteristics** for science missions and are used for solar physics, heliophysics, astrophysics, infrared astronomy, and space weather monitoring

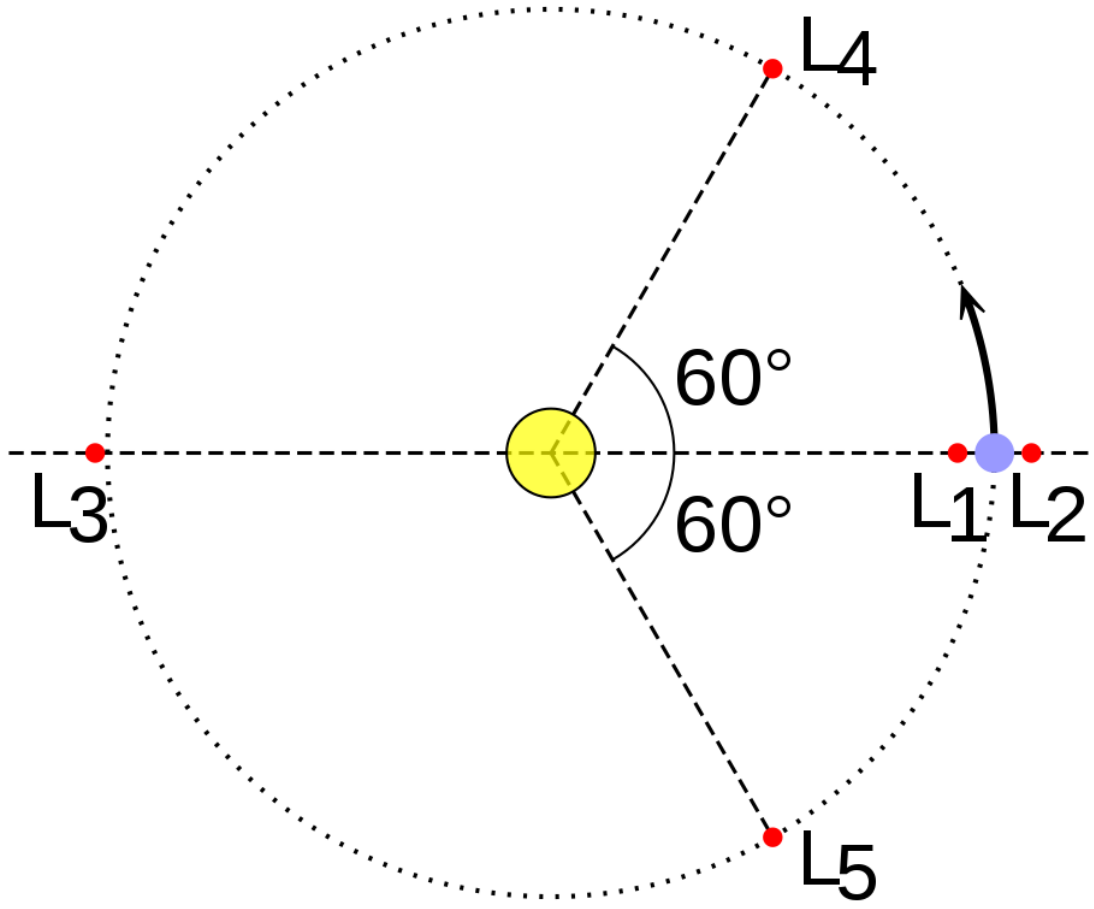

Sun-Earth Lagrange Point Missions

Past

Mission	Operator	Dates	LX Point
ISEE-3	NASA	08/1978 – 05/1997	L1, L2 transit
Geotail	ISAS/NASA	07/1992 - 06/2022	L2 transit
WMAP	NASA	06/2001 – 10/2010	L2
Genesis	NASA	08/2001 – 09/2004	L1
Spitzer Space Telescope	NASA	08/2003 – 01/2020	L5 transit
Herschel	ESA	05/2009 – 06/2013	L2
Planck	ESA	05/2009 – 10/2013	L2
Chang'e 2	CNSA	10/2010 – 2014	L2
Lisa Pathfinder	ESA	12/2015 – 06/2017	L1
Eddington	ESA	Cancelled 2003	L2
Terrestrial Planet Finder	NASA	Cancelled 2011	L2
Solar Cruiser	NASA	Cancelled 2022	Sub-L1

Current

Mission	Operator	Dates	LX Point
Wind	NASA	11/1994 -	L1
SOHO	ESA	12/1995 -	L1
ACE	NASA	08/1997 -	L1
STEREO A	NASA	10/2006 -	L4,L3,L5 transit
STEREO B	NASA	10/2006 – 10/2018	L5,L3,L4 transit
Gaia	ESA	12/2013 -	L2
Hayabusa2	JAXA	12/2014 -	L5 transit
DSCOVR	NOAA	02/2015 -	L1
OSIRIS-REX	NASA	09/2016 -	L4 transit
Spektr-RG	IKI/DLR	07/2019 -	L2
Chang'e 5	CNSA	11/2020 -	L1
JWST	NASA/ ESA/CSA	12/2021 –	L2

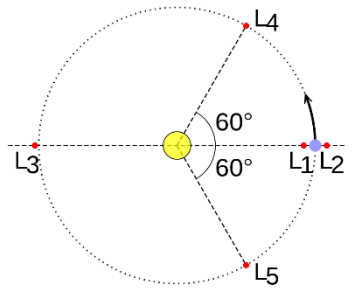

Future

Mission	Operator	Dates	LX Point
Aditya-L1	ISRO	2023 (plan)	L1
Euclid	ESA	2023 (plan)	L2
IMAP	NASA	2025 (plan)	L1
SWFO-L1	NOAA	2025 (plan)	L1
Vigil	ESA	Mid 2020's	L5
PLATO	ESA	2026 (plan)	L2
RST	NASA	2027 (plan)	L2
NEO Surveyor	NASA	2028 (plan)	L1
LiteBIRD	JAXA	2028 (plan)	L2
ARIEL	ESA	2029 (plan)	L2
Comet Interceptor	ESA/JAXA	2029 (plan)	L2 parked
ATHENA	ESA	2035 (plan)	L2
HabEx*	NASA	2035 (pro)	L2
OST*	NASA	2035 (pro)	L2
Lynx*	NASA	2036 (pro)	L2
LUVIOR*	NASA	2039 (pro)	L2
*Competing proposals			

L2 Plasma Environments

- Sun-Earth L1, L3, L4, L5 are in solar wind 100% of the time
- Sun-Earth L2 is located nominally near edge of magnetotail with magnetosheath encounters, solar wind is rare
- Large halo orbits used for L2 missions are typically in the magnetosheath and solar wind, magnetotail encounters are rare
- Lunar orbits including Earth-Moon L1, L2, …, L5 all pass through the magnetosheath and magnetotail once a month but spend most time (~75% in solar wind)

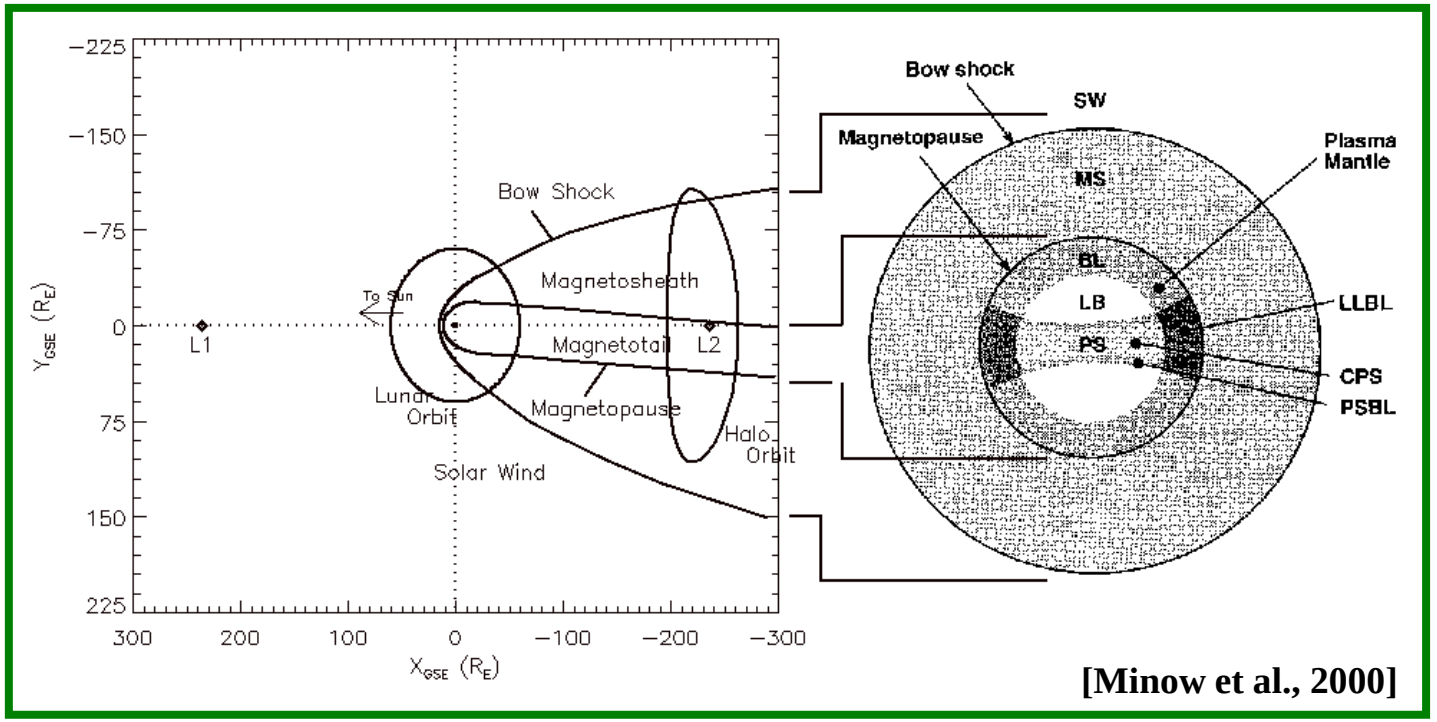

[Minow et al., 2000]

L2-CPE Environments	
SW	solar wind
MS	magnetosheath
PM	plasma mantle, lobes, boundary layers
PS	plasmasheet

JWST Sun-Earth L2 Mission Trajectory

- L2 missions typically use large halo or Lissajous orbits about L2
- Z-max is 520,000 km (81.6 Re)
- Range of y values is about 750,000 km (117.7 Re)

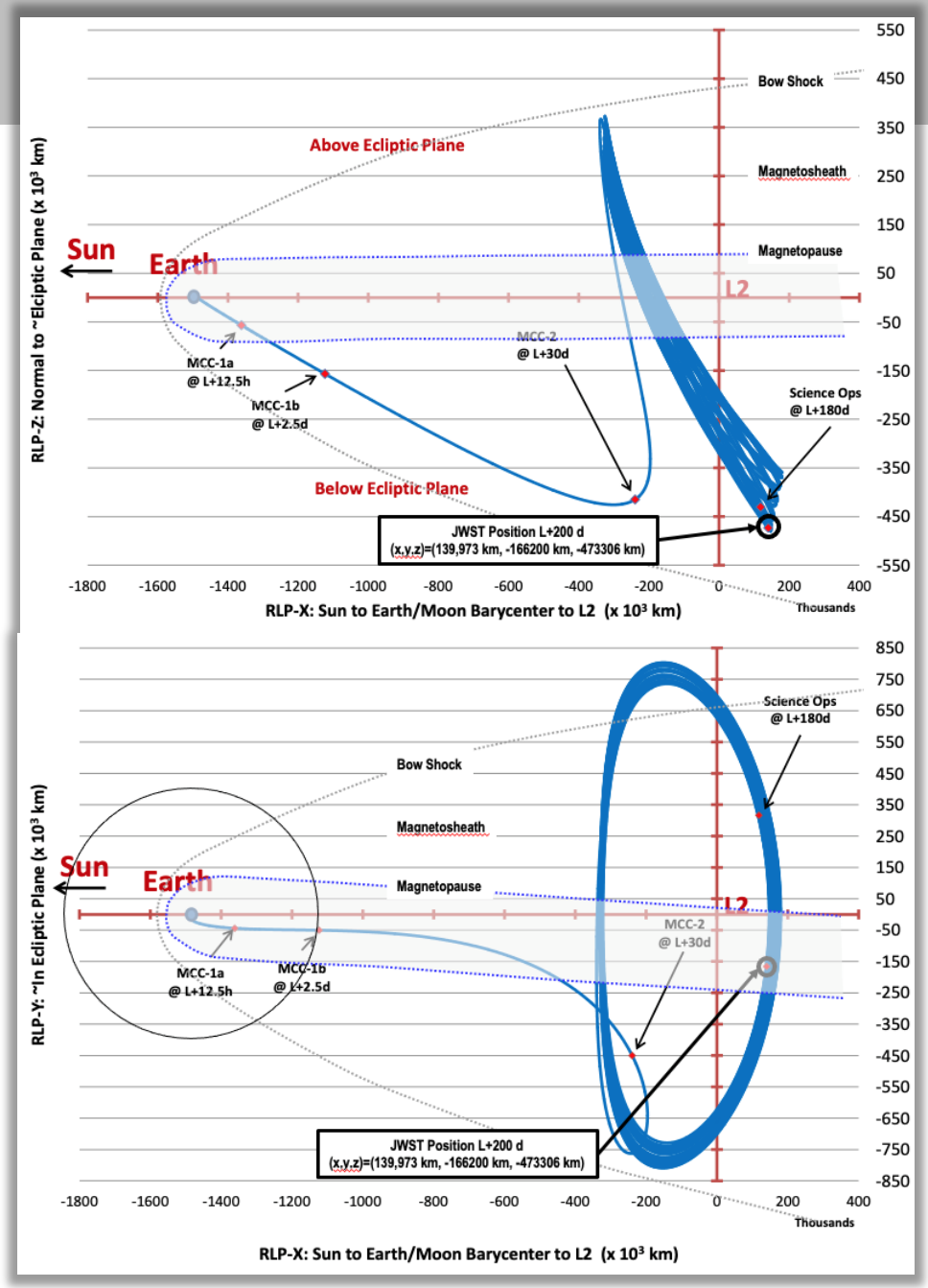

https://jwst-docs.stsci.edu/jwst-observatory-characteristics/jwst-orbit

L2-Charged Particle Environment (L2-CPE) Model

- L2-CPE generated to estimate radiation dose to surfaces of JWST while in orbit about the Sun-Earth L2 point

- Applicable for +100 Re ≥ Xgse ≥ -300 Re and radial distances ≥ 50 Re from Earth

- Funding provided by:
  - JWST Program
  - Space Environments and Effects Program
  - MSFC Engineering Directorate
  - Gateway
  - NESC

- Model options include
  - Particle flux in SW, MS, PS, and PM plasma regimes
  - Particle fluence accumulated over mission trajectory
    - Halo orbit generator
    - User provided trajectory
  - Plot generation
  - Scene generator

- Particle fluence is the feature of interest to our applications today since it generates the environments needed for computing radiation dose

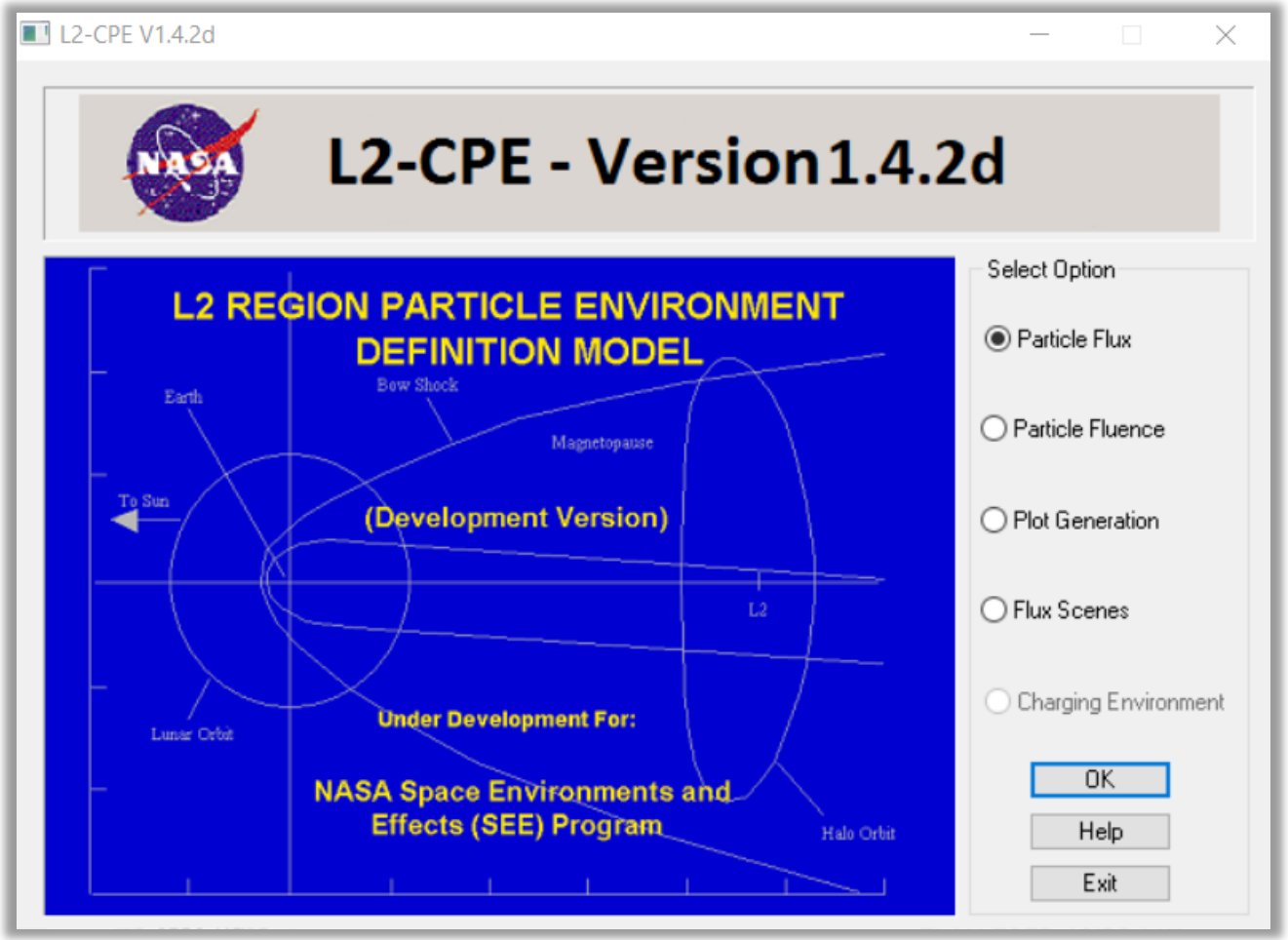

L2-CPE Fluence

- Species: electron, proton, helium (or all species)
- Energy range: 1 eV to 1 MeV
- Trajectory:
  - Model generated halo orbit (Z_{GSE} amplitude and scale factors to adjust halo dimensions)
  - User provided predefined orbit (trajectory)
- Fluence directions to surfaces in 6 orthogonal directions (GSE coordinates):
  - -X (sun facing), +X (anti-sun facing), +/-Y, +/- Z
- Reconstructed distributions: Maxwellian, Kappa
- IMP-8, Ulysses solar wind databases drive orientation and dimensions of the magnetosheath and magnetotail at each time step
  - IMP-8 Solar maximum (1992)
  - IMP-8 Solar minimum (1995)
- Plasma environments: solar wind (IMP-8, Ulysses scaled to 1 AU), magnetosheath (Geotail), magnetotail (Geotail)

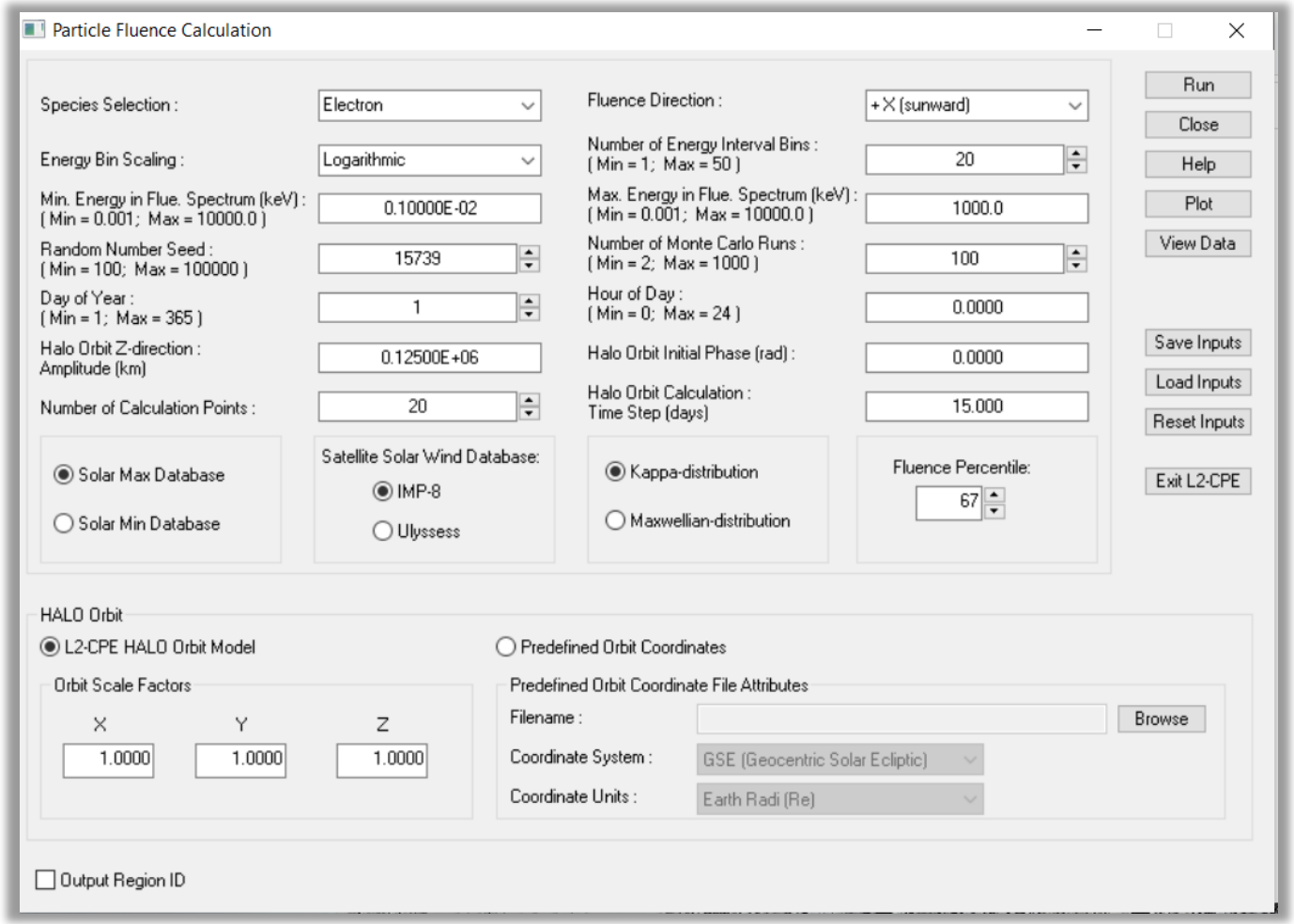

Magnetotail Aberration

- Solar wind drives magnetotail orientation
- Average aberration angle ~4° from Sun-Earth line

$$\theta \sim \text{atan}(V_E/V_{SW}) \sim \text{atan}(30 \text{ km s}^{-1}/468 \text{ km s}^{-1}) = 3.67°$$

- Spacecraft in orbit about L2 samples a range of plasma environments depending on (1) solar wind variability and (2) orbital motion

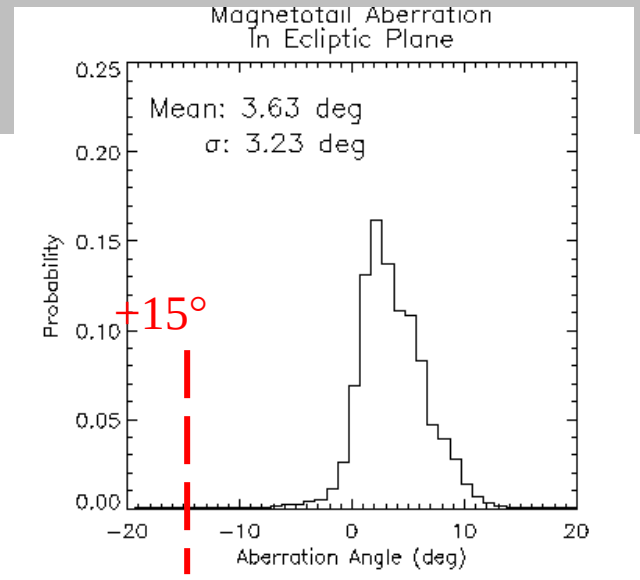

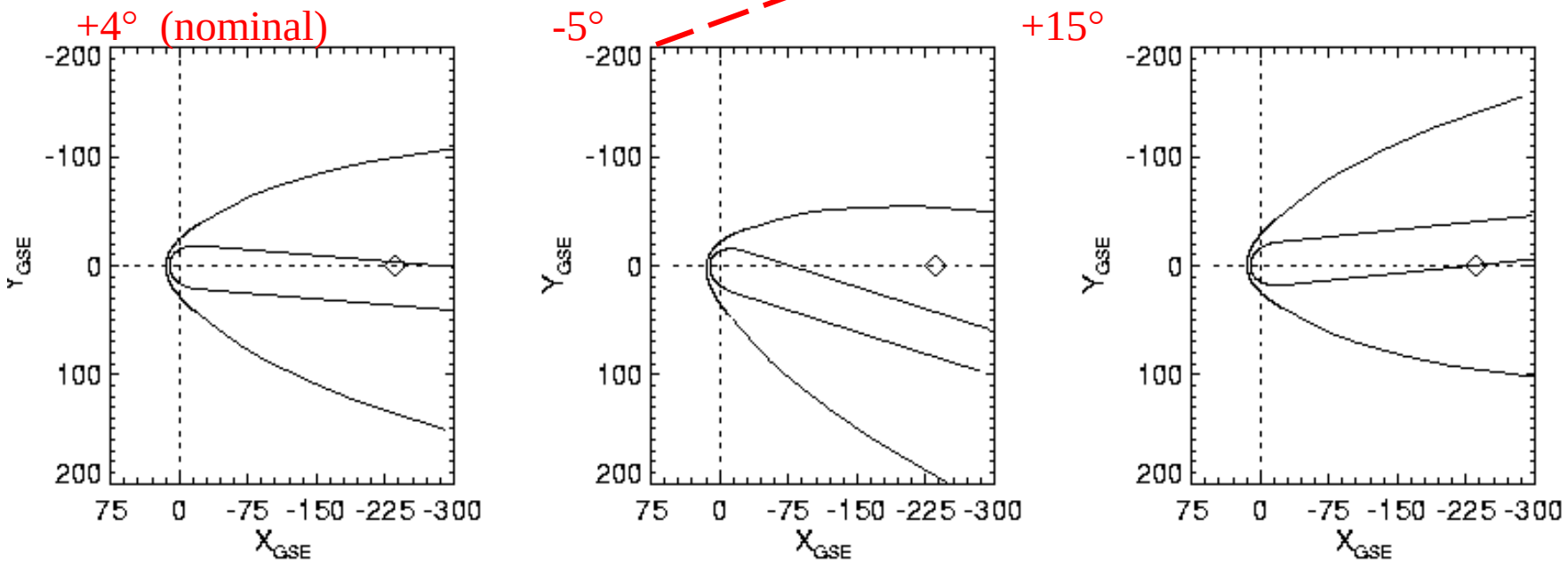

Nov 1973 - Dec 1998 IMP-8 solar wind data

[Blackwell et al., 2000]

Bow Shock and Magnetopause Variability

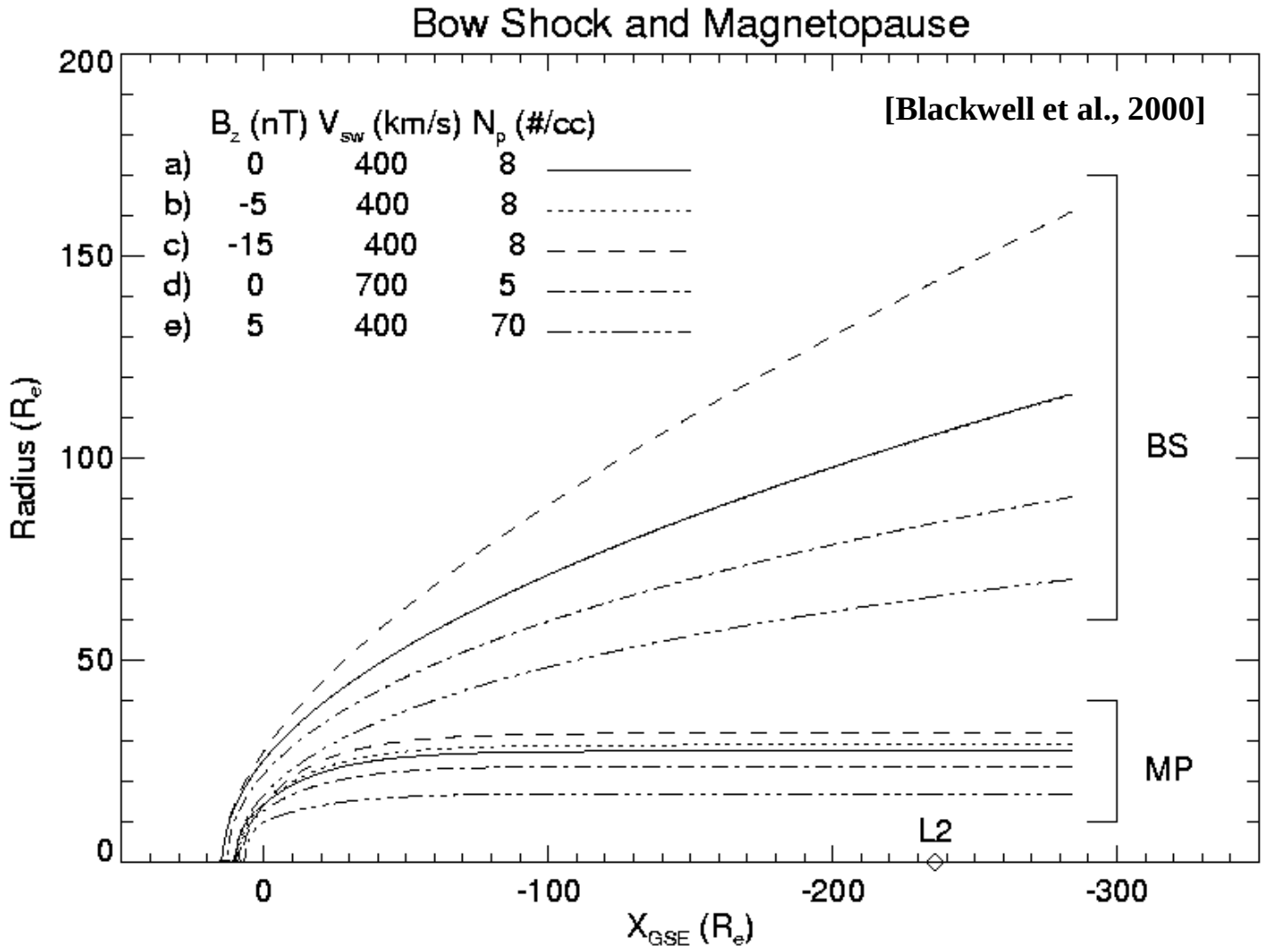

***Bennett* et al. [1997] bow shock**

***Petrinic and Russell* [1993, 1996] magnetopause**

IMP-8 plasma parameters with mean Parker spiral orientation for IMF provide variations in bow shock, magnetopause orientation and dimensions

Data Sources

Spacecraft/Instrument	Application	Source
Geotail	**magnetotail, magnetosheath**	
10 Re x 210 Re, near ecliptic		
• Comprehensive Plasma Instrument/Hot Plasma Analyzer (CPI/HPA)	core plasma moments	University of Iowa
• Energetic Particle and Ion Composition/Ion Composition Subsystem (EPIC/ICS)	non-thermal ion, electron flux	JHU/APL (ions) NSSDC/JHU/APL (electrons)
• Geotail plasma regime identification	database organization	EPIC Science Team, JHU/APL
IMP-8	**solar wind**	
~35 Re circular, near ecliptic		
• MIT Faraday Cup	core plasma moments	MIT
• Magnetic Field Experiment	interplanetary magnetic field	NSSDC (GSFC)
Ulysses	**solar wind**	
1 to 5.5 AU, 1.3 AU x 5.4 AU, 78º inclination		
• Solar Wind Observations Over the Poles of the Sun (SWOOPS)	core/halo electron moments core ion moments	NSSDC/SwRI
• Low Energy Magnetic Spectrometer (LEMS)	non-thermal ion, electron flux	NSSDC/Lucent Technologies
• Low Energy Foil Spectrometer (LEFS)	non-thermal ion, electron flux	NSSDC/Lucent Technologies

Plasma Regime Identification

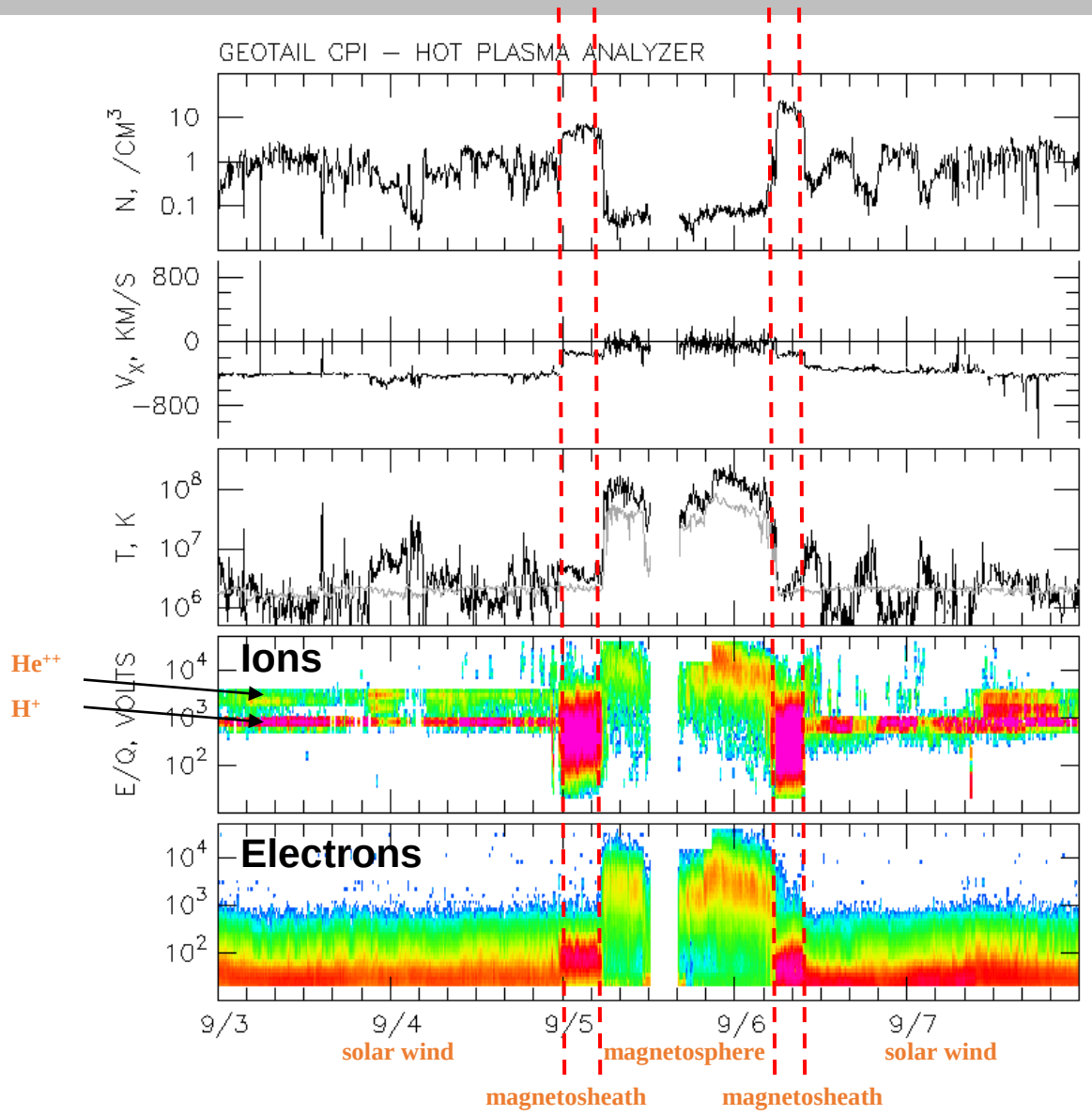

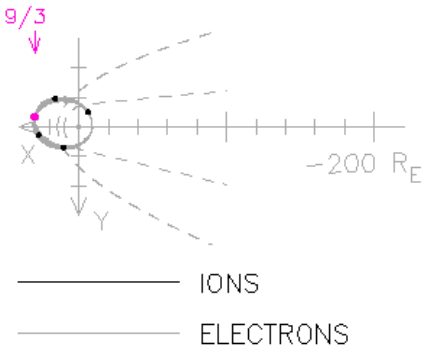

Near Earth plasma regimes are well ordered at low energies

Relatively easy to identify bow shock and magnetopause, plasma regimes by plasma characteristics

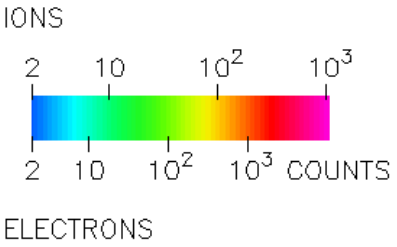

Geotail/CPI:
http://www-pi.physics.uiowa.edu/cpi/

Magnetotail Plasma at Lunar Distances

- Lunar plasma environment includes encounters with magnetotail and magnetosheath
- High temperature, low density plasma environments in magnetotail

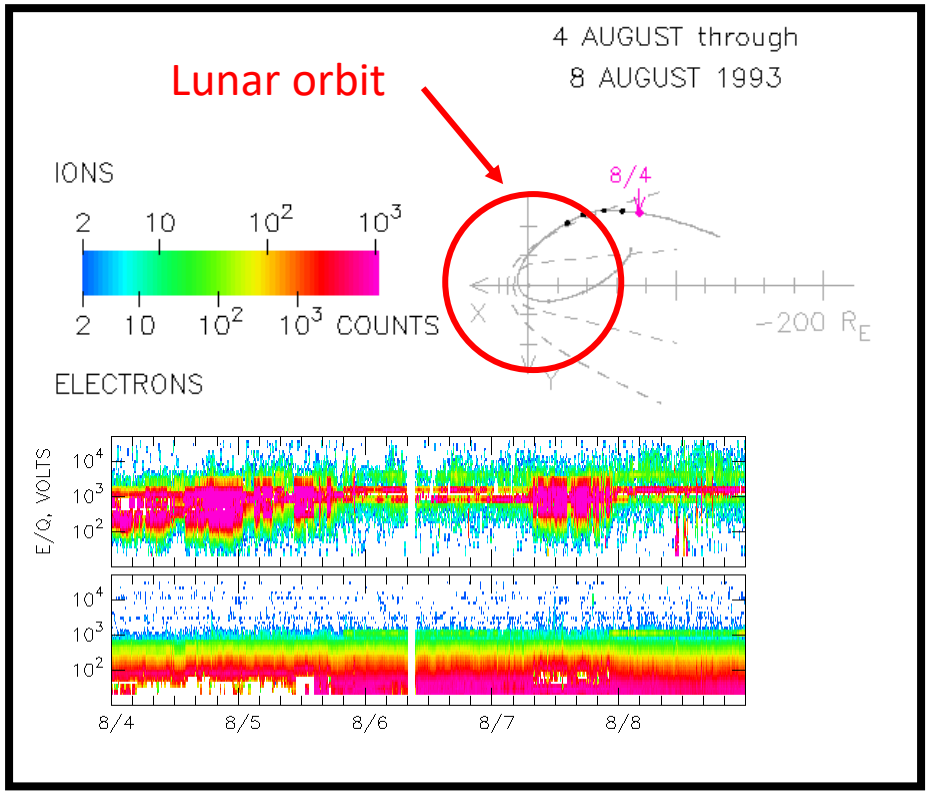

(Univ. of Iowa)

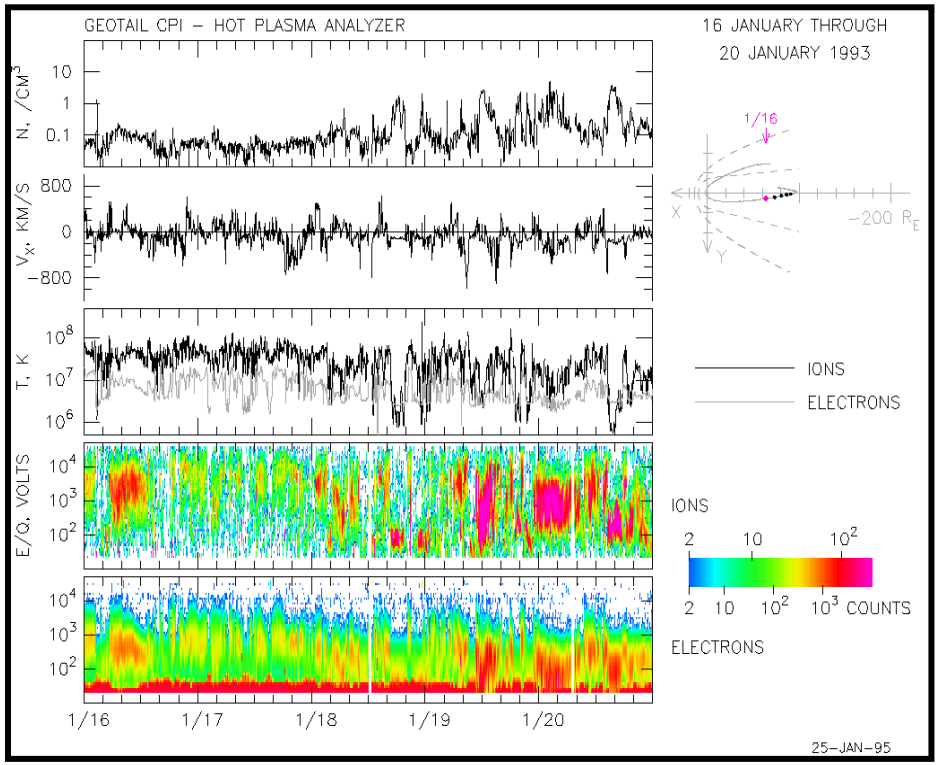

Geotail/CPI:
http://www-pi.physics.uiowa.edu/cpi/

Distant Magnetotail Environments

Identification of distant magnetotail plasma regimes is a challenge but plasma properties can be used to characterize plasma regimes into solar wind, magnetosheath, plasma mantle, boundary layer, and plasma sheet even at L2 distances

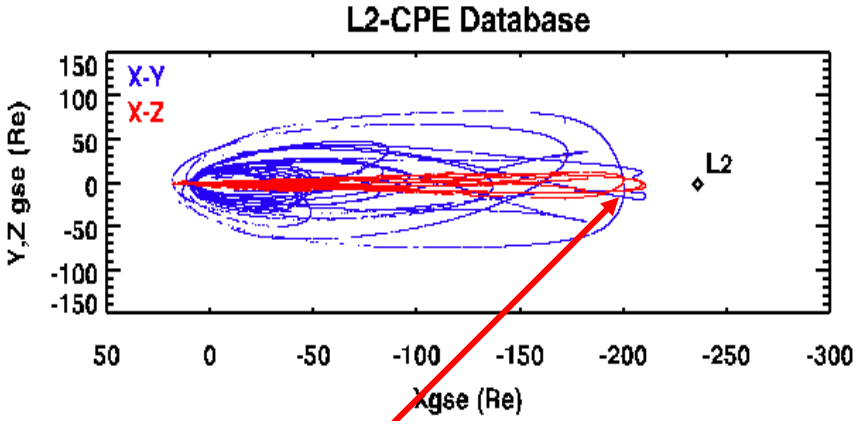

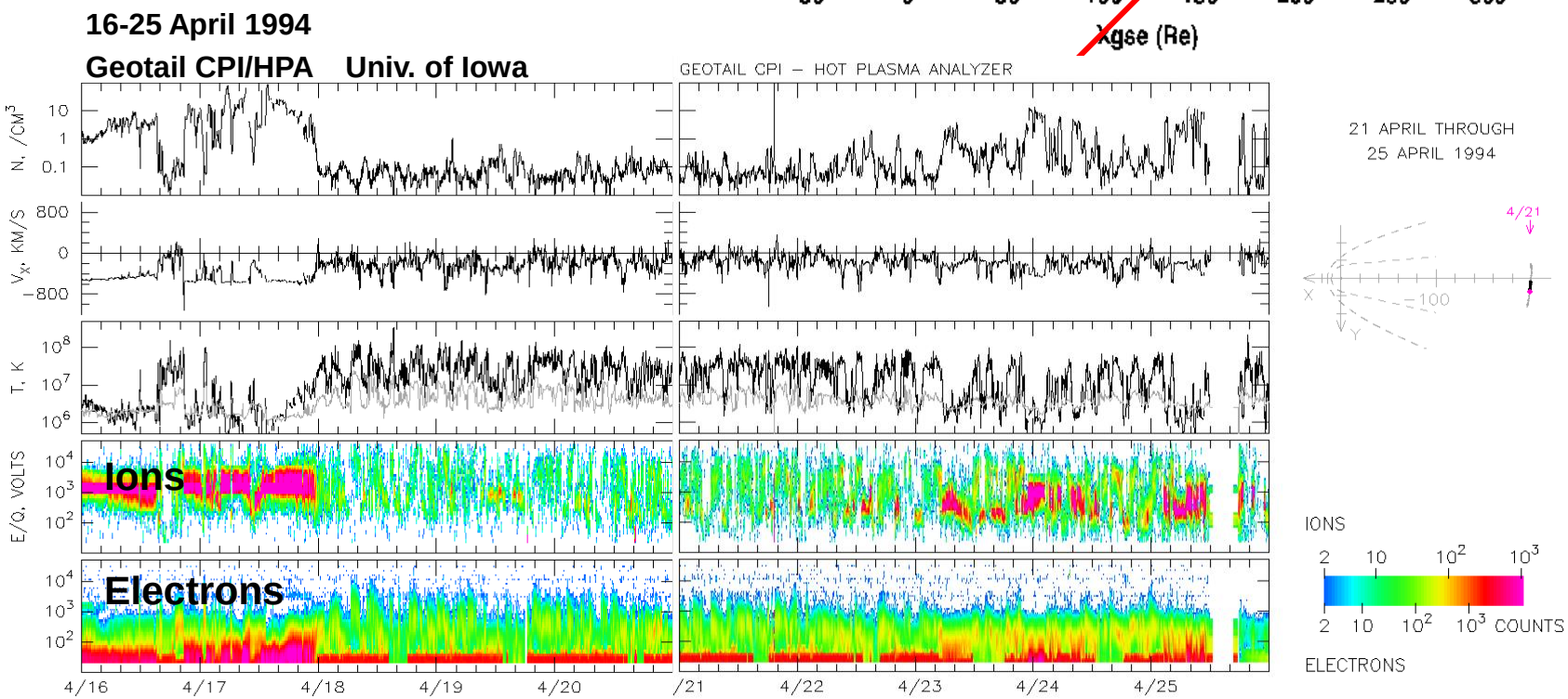

X_{GSE} ~ -200 Re 25 RE > Y_{GSE} > 0 Re

Geotail/CPI:
http://www-pi.physics.uiowa.edu/cpi/

EPIC Science Team Region Identifications

- EPIC* Science Team plasma regime identifications (RID) for 1 Oct 1992 through 31 Oct 1994 [*Eastman et al.*, 1998; *Christon et al.*, 1998] are adopted for L2-CPE
- Geotail records (CPI/HPA moments, EPIC flux) time tags compared to regime identification file to determine into which plasma regime database (SW, MS, PM, or PS) to place the record in the model

Geotail Regime IDs for: 94-106 0000 to 94-115 0000

Start Date/Time	End Date/Time	Interval minute	Kp min	Kp avg	Kp max	Start_Pos_(GSE Re) X	Start_Pos_(GSE Re) Y	Start_Pos_(GSE Re) Z	Stop_Pos_(GSE Re) X	Stop_Pos_(GSE Re) Y	Stop_Pos_(GSE Re) Z	Region = ## Notes
94-105 2016	94-106 0805	709	*2.7*	*3.5*	*3.7*	*-196.6*	*28.0*	*-5.1*	*-196.8*	*26.8*	*-4.7*	*MS = 44*
94-106 0805	*94-106 0814*	*9*	*3.3*	3.3	3.3	-196.8	26.8	-4.7	-196.8	26.8	-4.7	BL/MS = 34
94-106 0814	94-106 0928	74	2.3	2.8	3.3	-196.8	26.8	-4.7	-196.9	26.7	-4.7	MS = 44 LEP Data gap: 0140-0142
94-106 0928	94-106 0940	12	2.3	2.3	2.3	-196.9	26.7	-4.7	-196.9	26.7	-4.7	MS/BL = 43
94-106 0940	94-106 1146	126	2.3	2.3	2.3	-196.9	26.7	-4.7	-196.9	26.5	-4.6	MS = 44
94-106 1146	94-106 1156	10	2.3	2.3	2.3	-196.9	26.5	-4.6	-196.9	26.4	-4.6	PS = 11
94-106 1157	94-106 1519	202	2.3	2.9	3.3	-196.9	26.4	-4.6	-197.0	26.1	-4.5	MS = 44 LEP Data gap: 1245-1251
94-106 1520	94-106 1531	11	3.3	3.3	3.3	-197.0	26.1	-4.5	-197.0	26.1	-4.5	PS = 11 PSBL after 1528
94-106 1532	94-106 1551	19	3.3	3.3	3.3	-197.0	26.1	-4.5	-197.0	26.1	-4.5	BL = 33
94-106 1552	94-106 1611	19	3.3	3.3	3.3	-197.0	26.1	-4.5	-197.0	26.0	-4.5	PS = 11

*Energetic Particles and Ion Composition (EPIC) instrument

Geotail Differential Flux Reconstruction

- Charged particle flux for plasma environments was reconstructed from plasma moments, energetic particle flux measurements
- Geotail Comprehensive Plasma Instrument (CPI) Hot Plasma Analyzer (HPA) plasma moments provide low energy environments
- κ parameter constrained by matching Energetic Particle and Ion Composition (EPIC) Ion Composition Subsystem (ICS) differential ion flux, integral electron flux measurements
- Ions in 16 azimuths, electrons are spin averaged

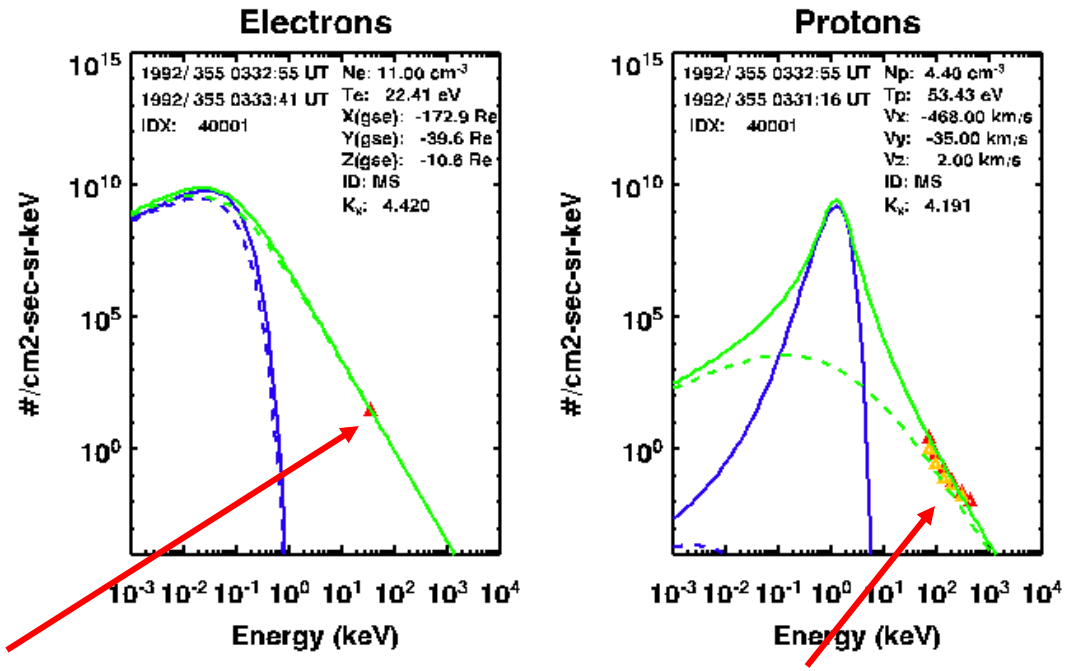

EPIC/ICS E>38 keV electrons

EPIC/ICS protons

Maxwellian differential flux distributions

$$f(\mathbf{v}) = \frac{n_o}{\left(\sqrt{\pi}\theta_{MB}\right)^3} \exp\left[-\frac{(\mathbf{v}-\mathbf{u})^2}{\theta_{MB}^2}\right] \qquad \theta_{MB} = \sqrt{\frac{2k_B T_i}{m_i}}$$

Kappa differential flux distributions

$$f(v) = \frac{n_o}{\left(\sqrt{\pi}\theta_\kappa\right)^3} \frac{\Gamma(\kappa+1)}{\sqrt{\kappa^3}\Gamma(\kappa-\frac{1}{2})}\left[1+\frac{v^2}{\kappa\theta_\kappa{}^2}\right]^{-\kappa-1} \qquad \theta_\kappa = \sqrt{\frac{(2\kappa-3)k_B T}{\kappa m}}, \qquad \kappa > \frac{3}{2}$$

Ulysses Differential Flux Reconstruction

- Charged particle flux for plasma environments was reconstructed from plasma moments, energetic particle flux measurements
- Ulysses Solar Wind Over the Poles of the Sun (SWOOPS) plasma moments provide low energy environments
- κ parameter constrained by matching Low Energy Magnetic Spectrometer (LEMS), Low Energy Foil Spectrometer (LEFS) differential flux measurements
- LEMS (LEFS) at 30º, 120º (60º, 150º) from Ulysses spin axis

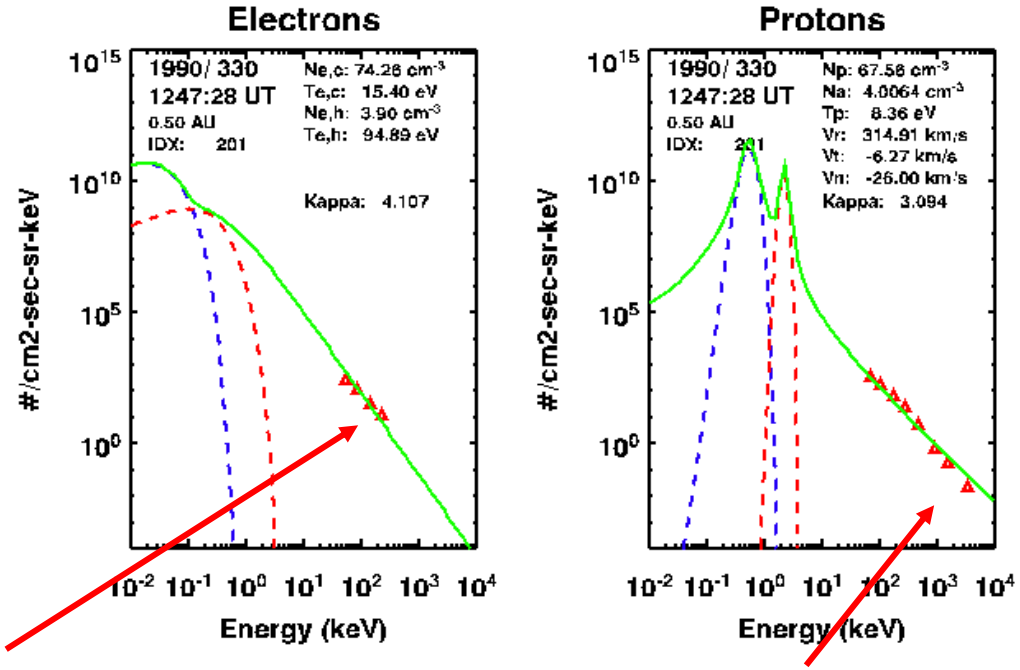

LEMS, LEFS electrons **LEMS, LEFS protons**

Maxwellian differential flux distributions

$$f(\mathbf{v}) = \frac{n_o}{\left(\sqrt{\pi}\theta_{MB}\right)^3} \exp\left[-\frac{(\mathbf{v}-\mathbf{u})^2}{\theta_{MB}^2}\right] \qquad \theta_{MB} = \sqrt{\frac{2k_B T_i}{m_i}}$$

Kappa differential flux distributions

$$f(v) = \frac{n_o}{\left(\sqrt{\pi}\theta_\kappa\right)^3} \frac{\Gamma(\kappa+1)}{\sqrt{\kappa^3}\Gamma(\kappa-\frac{1}{2})}\left[1+\frac{v^2}{\kappa\theta_\kappa{}^2}\right]^{-\kappa-1} \qquad \theta_\kappa = \sqrt{\frac{(2\kappa-3)k_B T}{\kappa m}}, \qquad \kappa > \tfrac{3}{2}$$

Kappa Flux Reconstruction Process

- Kappa differential number flux generation process:
  1) Compute Kappa distribution functions from plasma moments, initial guess for κ parameter
  2) Compute differential flux J from distribution functions f using the relationship $J = p^2 f$
  3) Differential flux at energies of 10's to 100's keV is compared to flux measurements
  4) If measured and computed flux is not within specified error tolerance, adjust κ parameter and repeat steps 1 to 3 are repeated

- The iterative process is used to obtain a κ parameter which gives the best differential flux based on comparison with measured differential flux

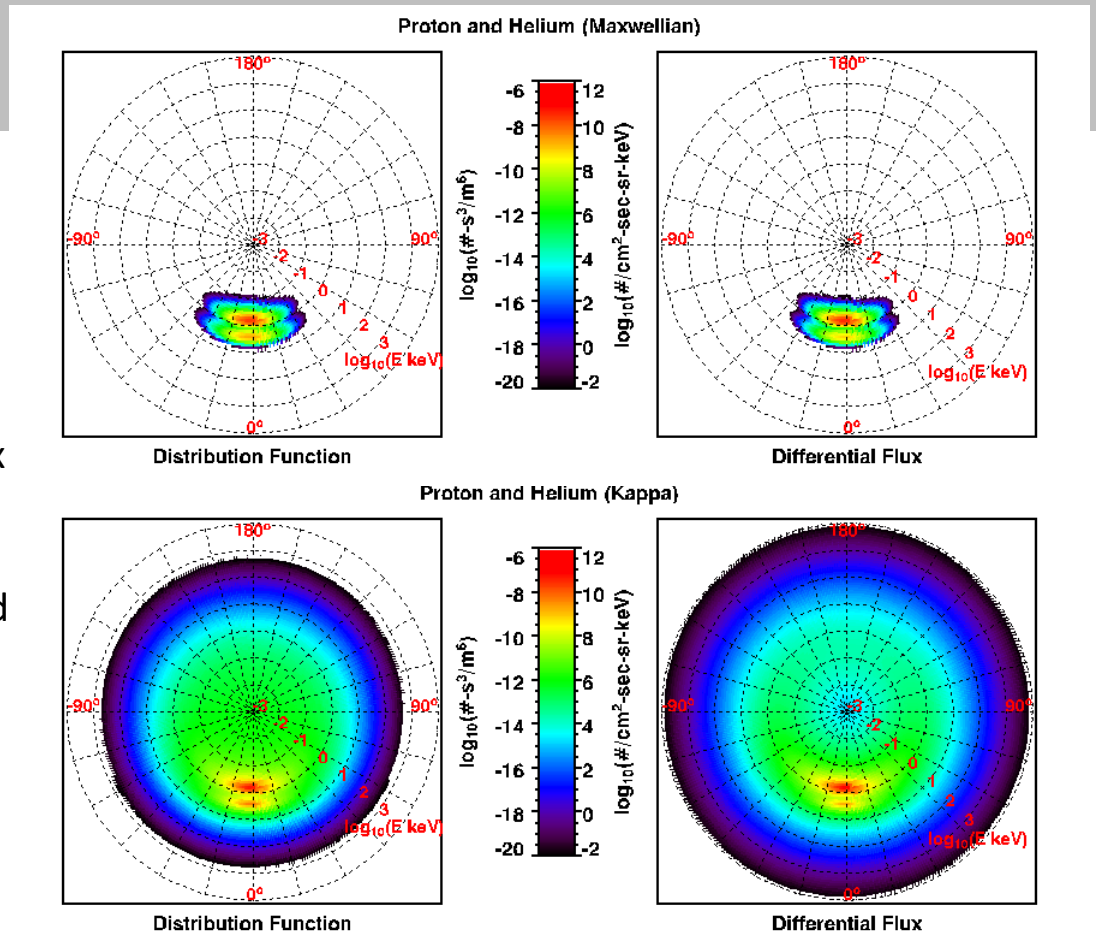

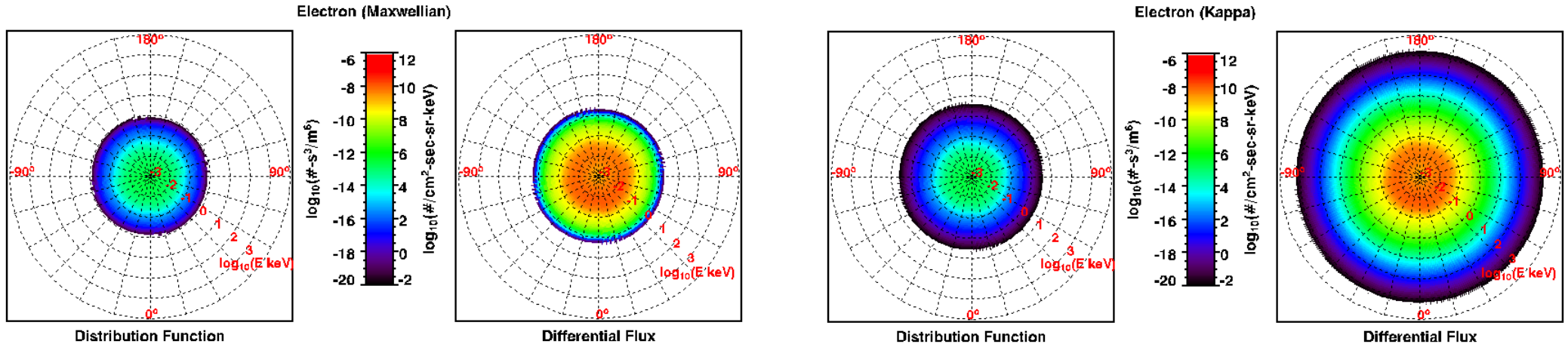

L2-Charged Particle Environment (L2-CPE) Model

- Original L2-CPE engineering model of L2 free field plasma environments applicable to:
  - $-100\ R_E < X_{GSE} < 300\ R_E$
  - ~0.1 keV < E < ~1 MeV
  - H^+, He^{++}, e^-
- Based on in-situ satellite measurements of plasma (<1 MeV) properties in solar wind, magnetosheath, and magnetotail plasma regimes
- Solar wind, magnetosheath, and magnetotail plasma environments ordered by solar wind dependent bow shock and magnetopause boundaries
- Empirical model flux, fluence output traceable to measurements
- L2-CPE Model was developed by NASA to characterize the low energy charged particle environments of importance to thin materials used in construction of the James Webb Space Telescope

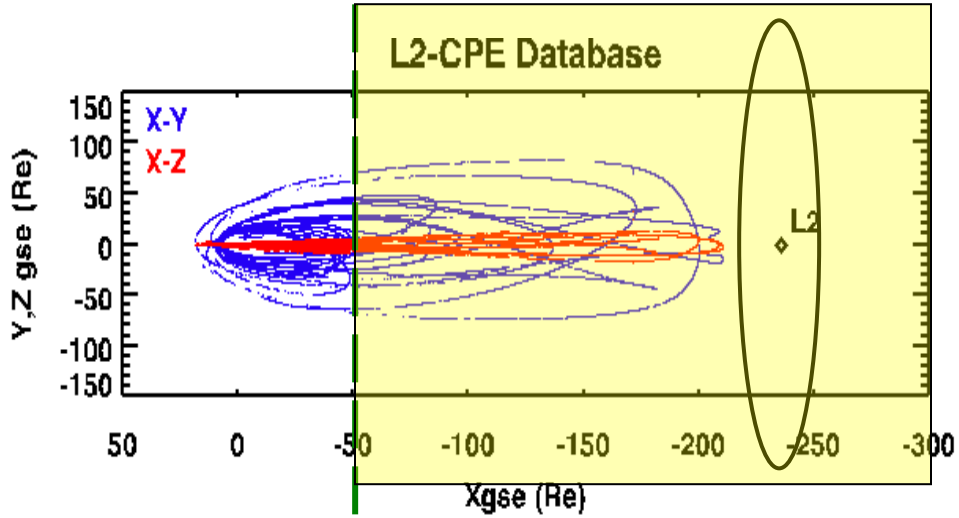

Only data with -50 Re > X used in model

L2-CPE includes complete 2+ years Geotail distant magnetotail records

L2-Charged Particle Environment (L2-CPE) Model

- Updated L2-CPE (V1.4.2d)* engineering model of L2 free field plasma environments applicable to:
  $+100\ R_E < X_{GSE} < 300\ R_E$
  ~0.1 keV < E < ~1 MeV
  H^+, He^{++}, e^-

- Based on in-situ satellite measurements of plasma (<1 MeV) properties in solar wind, magnetosheath, and magnetotail plasma regimes

- Solar wind, magnetosheath, and magnetotail plasma environments ordered by solar wind dependent bow shock and magnetopause boundaries

- Empirical model flux, fluence output traceable to measurements

- L2-CPE Model was developed by NASA to characterize the low energy charged particle environments of importance to thin materials used in construction of the James Webb Space Telescope

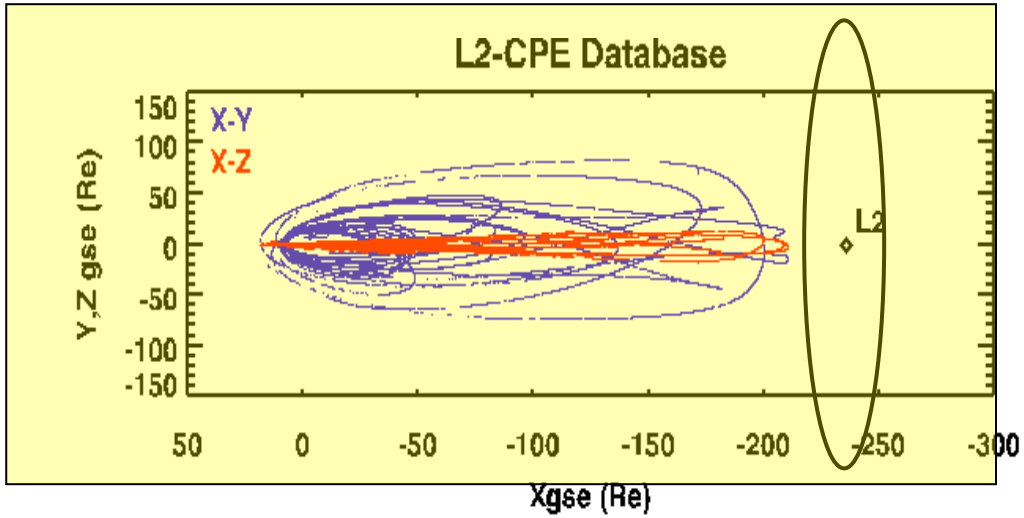

Only data with -50 Re > X used in model

L2-CPE includes complete 2+ years Geotail distant magnetotail records

*Updated code can be used for all Lagrange points as well as lunar orbit

Example: 60-Re Z-Amplitude Halo Orbit

- FLU_aa_ELEXPOS
- FLU_ab_ELEXNEG
- FLU_ac_ELEYPOS
- FLU_ad_ELEYNEG
- FLU_ae_ELEZPOS
- FLU_af_ELEZNEG
- FLU_ba_PROXPOS
- FLU_bb_PROXNEG
- FLU_bc_PROYPOS
- FLU_bd_PROYNEG
- FLU_be_PROZPOS
- FLU_bf_PROZNEG
- FLU_ca_HELXPOS
- FLU_cb_HELXNEG
- FLU_cc_HELYPOS
- FLU_cd_HELYNEG
- FLU_ce_HELZPOS
- FLU_cf_HELZNEG
- Flu_SATREG

FLU_ij_SPEKDIR.dat

i = a,b,c where
- a: electron
- b: proton
- c: helium

j = a,b,c where
- a: +X
- b: -X
- c: +Y
- d: -Y
- e: +Z
- f: -Z

SPE: electron, proton, helium

K= X, Y, Z

DIR: POS (+), NEG (-)

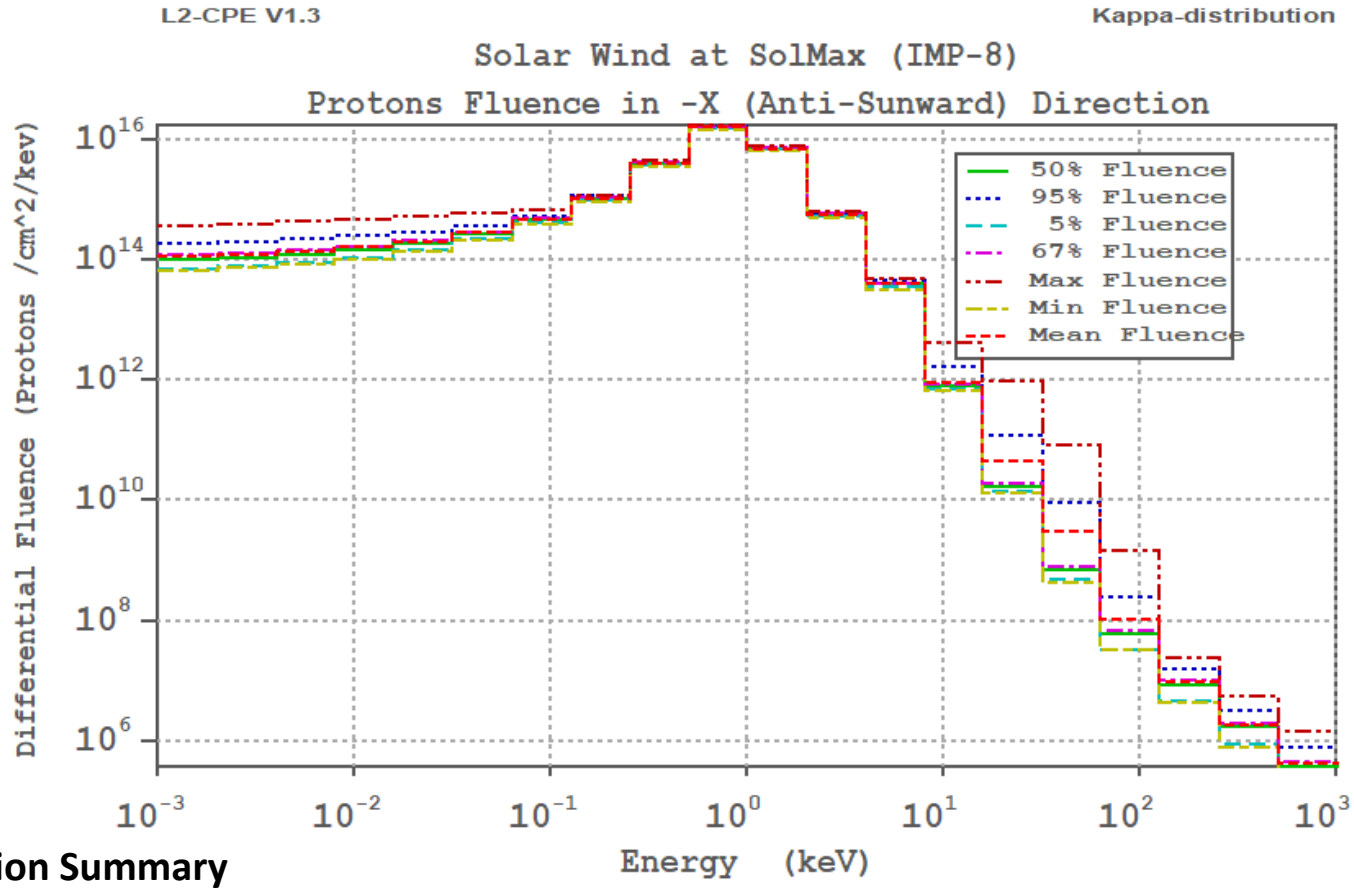

Satellite Region Summary

Number of Monte Carlo Runs = 100

Total duration of problem = 365.0000 days

Inside Solar Wind Region:	27.16 % of the time	(99.15 days)
Inside Plasma Sheet Region:	0.05 % of the time	(0.19 days)
Inside Plasma Mantle Region:	0.50 % of the time	(1.83 days)
Inside Magnetosheath Region:	72.28 % of the time	(263.83 days)

Example: 60-Re Z-Amplitude Halo Orbit

- Fluence file header provides
  - Distribution function used in reconstruction
  - Trajectory (halo or user provided)
  - Number of Monte Carlo runs
  - Species and flux direction in file
  - Energy range and number of bins
  - Integral fluence summary

- Plasma regime database is sampled by random draws for each Monte Carlo run

- Fluence statistics for integrated fluence in spectrum provided for
  - 50%
  - 5% and 95%
  - User selected percentile (67% used here)
  - Maximum and minimum
  - Mean and standard deviation

```
                    - FLUENCE SUMMARY -
 L2-CPE V1.3              Kappa-distribution
 Cartesian (LRAD) Algorithm
 HALO Orbit Model

 Number of Monte Carlo Runs =        100

 Species  =>  Protons
Solar Wind at SolMax (IMP-8)
 Negative X direction fluence calculated.

 Minimum Energy =     0.0010 keV
 Maximum Energy =  1000.0000 keV

 Number of Energy Bins   =    20

 50% Total Fluence       =   0.1792E+17 (#/cm^2)
 95% Total Fluence       =   0.1845E+17 (#/cm^2)
  5% Total Fluence       =   0.1724E+17 (#/cm^2)
  67% Total Fluence      =   0.1806E+17 (#/cm^2)
 Maximum Total Fluence   =   0.1867E+17 (#/cm^2)
 Minimum Total Fluence   =   0.1704E+17 (#/cm^2)
 Mean Total Fluence      =   0.1790E+17 (#/cm^2)
 Std. Dev. Total Fluence =   0.3489E+15 (#/cm^2)
```

Example: 60-Re Z-Amplitude Halo Orbit

Differential Energy Fluence Table (#/cm^2/keV)

E1(keV)	E2(keV)	50%	95%	5%	67%	Maximum	Minimum	Mean	Std. Dev.
0.0010	0.0020	0.1024E+15	0.1838E+15	0.7037E+14	0.1228E+15	0.3609E+15	0.6582E+14	0.1162E+15	0.4474E+14
0.0020	0.0040	0.1117E+15	0.1966E+15	0.7749E+14	0.1324E+15	0.3906E+15	0.7283E+14	0.1258E+15	0.4764E+14
0.0040	0.0079	0.1250E+15	0.2199E+15	0.8905E+14	0.1470E+15	0.4316E+15	0.8402E+14	0.1405E+15	0.5146E+14
0.0079	0.0158	0.1468E+15	0.2520E+15	0.1089E+15	0.1713E+15	0.4849E+15	0.1029E+15	0.1643E+15	0.5573E+14
0.0158	0.0316	0.1864E+15	0.2969E+15	0.1446E+15	0.2124E+15	0.5448E+15	0.1376E+15	0.2049E+15	0.5837E+14
0.0316	0.0631	0.2701E+15	0.3626E+15	0.2208E+15	0.2920E+15	0.6004E+15	0.2109E+15	0.2843E+15	0.5510E+14
0.0631	0.1259	0.4754E+15	0.5445E+15	0.4202E+15	0.4933E+15	0.6981E+15	0.3871E+15	0.4779E+15	0.4635E+14
0.1259	0.2512	0.1073E+16	0.1168E+16	0.9839E+15	0.1098E+16	0.1186E+16	0.9156E+15	0.1075E+16	0.5392E+14
0.2512	0.5012	0.4067E+16	0.4408E+16	0.3759E+16	0.4179E+16	0.4599E+16	0.3647E+16	0.4095E+16	0.1984E+15
0.5012	1.0000	0.1642E+17	0.1701E+17	0.1551E+17	0.1665E+17	0.1731E+17	0.1507E+17	0.1640E+17	0.4723E+15
1.0000	1.9953	0.7236E+16	0.7630E+16	0.6836E+16	0.7326E+16	0.7863E+16	0.6747E+16	0.7238E+16	0.2320E+15
1.9953	3.9811	0.5764E+15	0.6154E+15	0.5355E+15	0.5860E+15	0.6364E+15	0.5126E+15	0.5752E+15	0.2584E+14
3.9811	7.9433	0.3959E+14	0.4491E+14	0.3522E+14	0.4100E+14	0.4921E+14	0.3267E+14	0.3983E+14	0.3130E+13
7.9433	15.8489	0.8077E+12	0.1624E+13	0.7038E+12	0.8351E+12	0.4220E+13	0.6832E+12	0.9267E+12	0.4461E+12
15.8489	31.6228	0.1698E+11	0.1230E+12	0.1389E+11	0.1868E+11	0.9842E+12	0.1335E+11	0.4561E+11	0.1217E+12
31.6228	63.0957	0.6818E+09	0.8934E+10	0.4684E+09	0.7860E+09	0.8128E+11	0.4283E+09	0.3031E+10	0.1044E+11
63.0957	125.8925	0.5849E+08	0.2455E+09	0.3309E+08	0.6734E+08	0.1413E+10	0.3142E+08	0.1029E+09	0.1884E+09
125.8925	251.1887	0.8536E+07	0.1512E+08	0.4643E+07	0.9922E+07	0.2302E+08	0.4128E+07	0.9233E+07	0.3560E+07
251.1887	501.1873	0.1654E+07	0.3209E+07	0.8574E+06	0.1901E+07	0.5412E+07	0.7833E+06	0.1815E+07	0.7871E+06
501.1873	1000.0000	0.3716E+06	0.7503E+06	0.1819E+06	0.4333E+06	0.1376E+07	0.1614E+06	0.4132E+06	0.1968E+06

Example: Halo Orbit Trade Study

- L2-CPE provides a convenient method for estimating charged particle fluence to spacecraft surfaces in trade studies that vary mission duration and spacecraft trajectory
- L2CPE example* here shows variation in z-amplitude of halo orbit over a period of 365 days on the sun-facing surface
  - 50% total fluence in spectrum from 1 keV to 1 MeV for flux in –X direction (impacting sun-facing surface of spacecraft)
  - Output files contain the full spectral information for all species and direction, total integral fluence in spectrum used here is convenient method for comparing runs

Halo Orbit Z-Amplitude	Time in Plasma Regime (percent)				-X, 50% Total Fluence (#/cm2)		
	Solar Wind	M'sheath	P Mantle	P Sheet	e^-	H^+	He^{++}
10 Re	11.93%	74.88%	8.81%	4.37%	4.6e16	1.3e16	6.1e14
20 Re	13.09%	77.47%	5.98%	3.47%	4.8e16	1.3e16	6.5e14
40 Re	17.98%	78.45%	3.00%	0.57%	5.2e16	1.5e16	7.2e14
60 Re	27.16%	72.28%	0.50%	0.05%	5.6e16	1.8e16	8.4e14
80 Re	43.30%	56.61%	0.07%	0.02%	6.1e16	2.2e16	1.0e15
100 Re	61.63%	38.34%	0.02%	0.01%	6.5e16	2.5e16	1.2e15
150 Re	80.14%	19.85%	0.01%	0.00%	6.8e16	2.9e16	1.4e15
200 Re	88.41%	11.58%	0.00%	0.00%	7.0e16	3.1e16	1.4e15

*L2CPE options: Kappa, IMP-8, Solar Maximum, Halo Orbit, 3650 points with 0.1-day time steps, 100 Monte Carlo runs

Example: JWST Plasma Environment Probability

- JWST mission design trajectory
- Np = 99948, Monte Carlo = 1000
- JWST ephemeris uses variable time steps from 1 minute following launch to 4 days in orbit about L2
- Sampled trajectory using 0.04 days (0.96 hours) time steps to generate the L2-CPE input file with fixed time steps

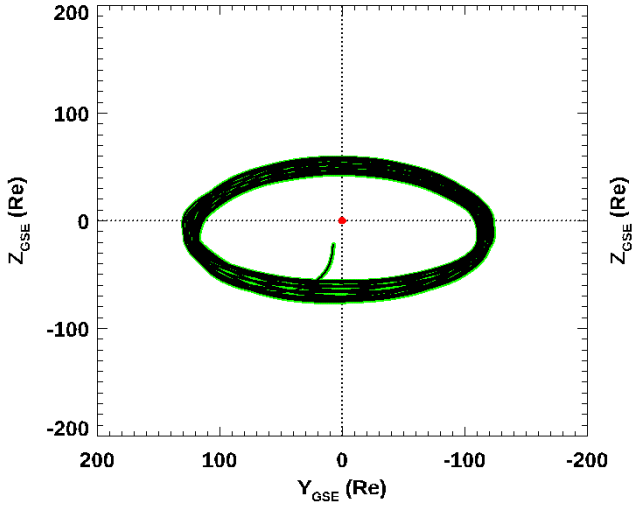

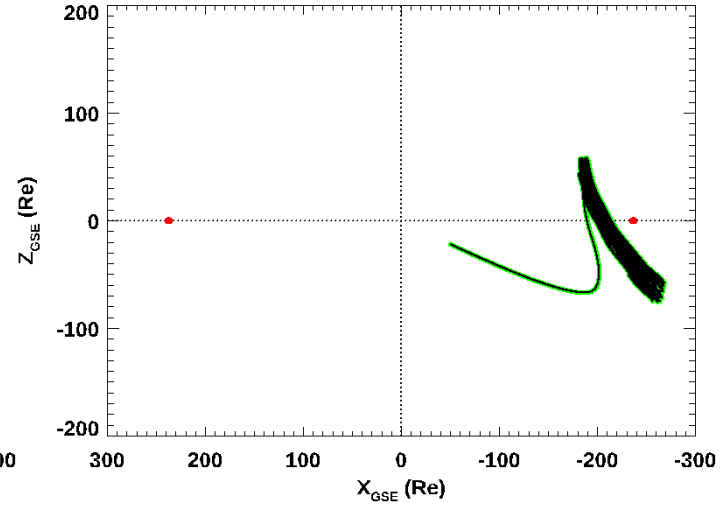

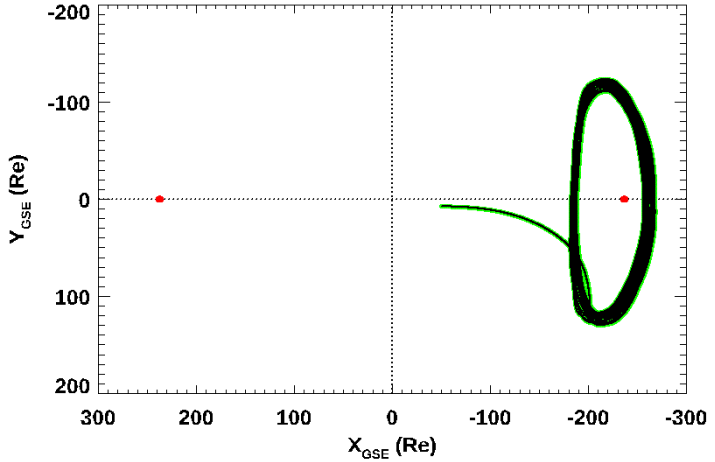

- SATELLITE LOCATION SUMMARY -

Number of Monte Carlo Runs = 1000
Total duration of problem = 3997.9199 days ~11 years

Inside Solar Wind Region:	33.28 % of the time	(1330.44 days)
Inside Plasma Sheet Region:	0.01 % of the time	(0.52 days)
Inside Plasma Mantle Region:	0.21 % of the time	(8.47 days)
Inside Magnetosheath Region:	66.50 % of the time	(2658.49 days)

Example: JWST Plasma Environment Probability

- 1000 MC runs allows probability of being located in a given plasma regime at each time step to be computed at the 0.1% level
- Plot only shows the first 500 days of the JWST trajectory
- L2-CPE and L2_REGION_STAT.pro provides the full mission trajectory including statistical estimates of plasma region encounters at each time step

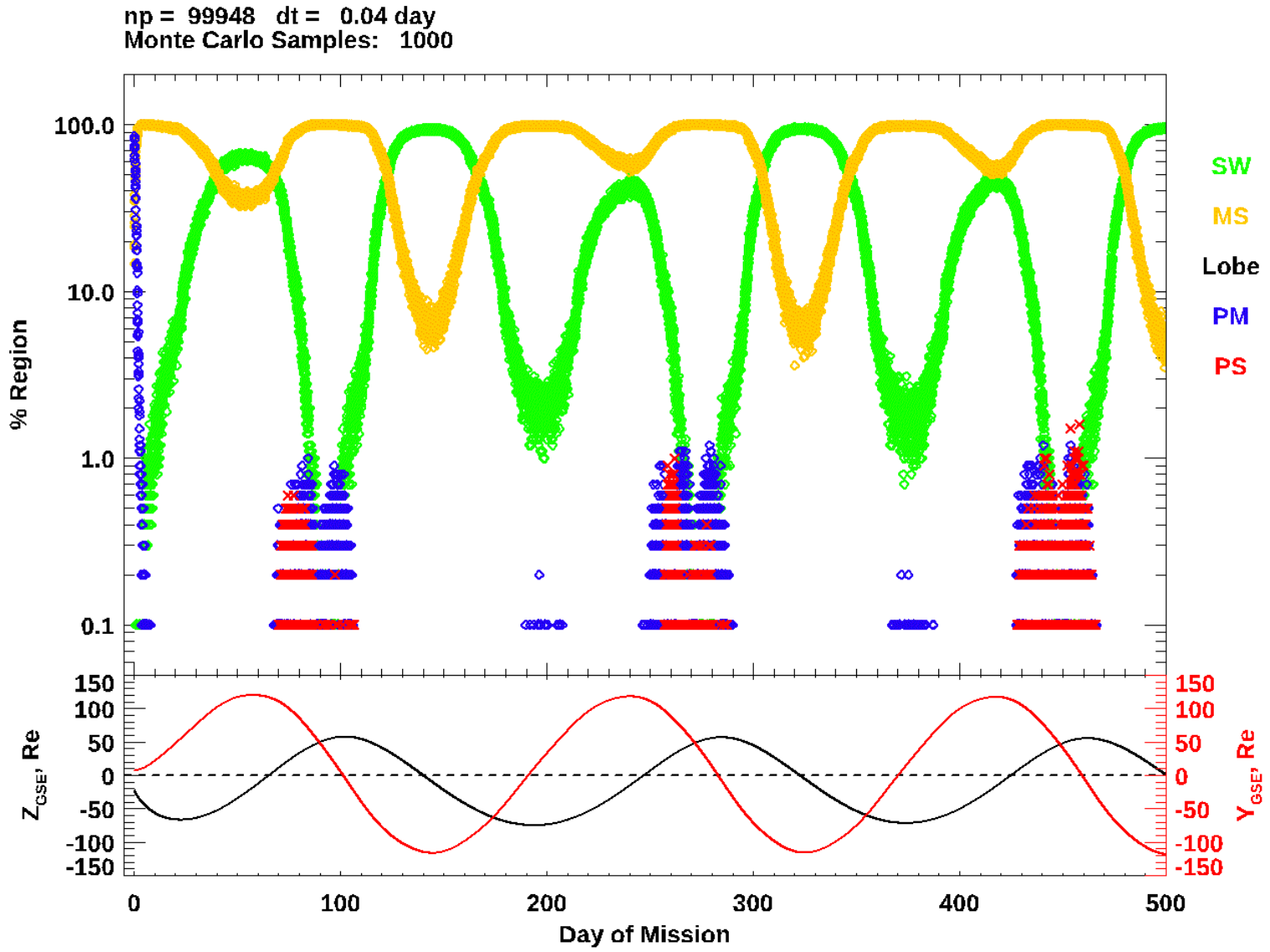

Radiation Transport Example: T300/Epoxy

- Radiation transport analysis using a T300 graphite/epoxy composite

- All three cases implemented as planar, tabular geometry files in MULASSIS Monte Carlo radiation transport code (implemented in https://www.spenvis.oma.be/)

- **Case A:** Pure resin (**Resin**)
  - Chemical formula -(C18H20-O3)-
  - Density 1.14 g/cm3
  - Configuration: Layers 1 through 20 are all resin

- **Case B:** Pure carbon fiber (**Carbon_fiber**)
  - Chemical formula C
  - Density 2.00 g/cm3
  - Configuration: Layers 1 through 20 are all carbon fiber

- **Case C:** T300 composite resin and carbon fiber coated with thin layer of pure resin (**T300**)
  - Chemical formula Resin: -(C18H20-O3)-
    Composite: -(C162-C18H20-O3)- 90% C and 10% resin
  - Density Resin: = 1.14 g/cm3
    Composite: = 0.9*2.00 g/cm3 + 0.1*1.14 g/cm3
    = 1.914 g/cm3
  - Configuration:
    - Layers 1 through 10 are pure resin (0.0 to 0.3 micron)
    - Layers 11 through 20 are 90% carbon fiber and 10% resin (0.3 to 3000 micron)

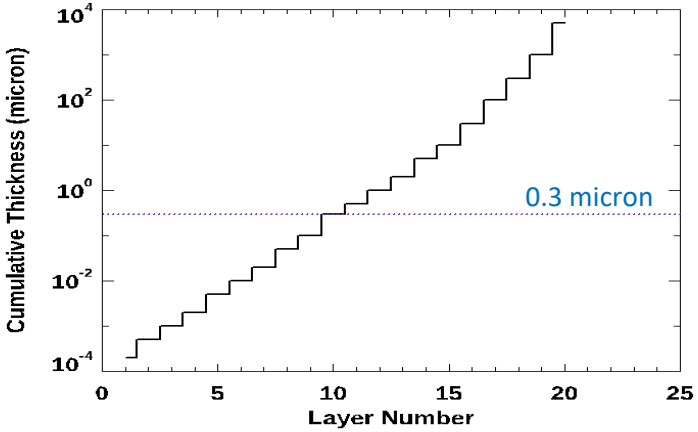

Layer Number	Layer Thickness (micron)	Cumulative Thickness (micron)
1	2.0000e-04	2.0000e-04
2	3.0000e-04	5.0000e-04
3	5.0000e-04	1.0000e-03
4	1.0000e-03	2.0000e-03
5	3.0000e-03	5.0000e-03
6	5.0000e-03	1.0000e-02
7	1.0000e-02	2.0000e-02
8	3.0000e-02	5.0000e-02
9	5.0000e-02	1.0000e-01
10	2.0000e-01	3.0000e-01
11	2.0000e-01	5.0000e-01
12	5.0000e-01	1.0000e+00
13	1.0000e+00	2.0000e+00
14	3.0000e+00	5.0000e+00
15	5.0000e+00	1.0000e+01
16	2.0000e+01	3.0000e+01
17	7.0000e+01	1.0000e+02
18	2.0000e+02	3.0000e+02
19	7.0000e+02	1.0000e+03
20	4.0000e+03	5.0000e+03

MULASSIS Geometry

Case A — Geometry: User defined

Shape: planar slab — Number of layers: 20

Layer number	Material	Thickness (unit)	Visualisation colour
Layer 1	Resin	2.0e-4 μm	white
Layer 2	Resin	3.0e-4 μm	white
Layer 3	Resin	5.0e-4 μm	white
Layer 4	Resin	1.0e-3 μm	white
Layer 5	Resin	3.0e-3 μm	white
Layer 6	Resin	5.0e-3 μm	white
Layer 7	Resin	1.0e-2 μm	white
Layer 8	Resin	3.0e-2 μm	white
Layer 9	Resin	5.0e-2 μm	white
Layer 10	Resin	2.0e-1 μm	white
Layer 11	Resin	2.0e-1 μm	white
Layer 12	Resin	5.0e-1 μm	white
Layer 13	Resin	1.0 μm	white
Layer 14	Resin	3.0 μm	white
Layer 15	Resin	5.0 μm	white
Layer 16	Resin	20.0 μm	white
Layer 17	Resin	70. μm	white
Layer 18	Resin	200. μm	white
Layer 19	Resin	700. μm	white
Layer 20	Resin	4000. μm	white

Visualisation

Format: Encapsulated PostScript (EPS)

Particle tracks: Display

Case B — Geometry: User defined

Shape: planar slab — Number of layers: 20

Layer number	Material	Thickness (unit)	Visualisation colour
Layer 1	Carbon_fiber	2.0e-4 μm	white
Layer 2	Carbon_fiber	3.0e-4 μm	white
Layer 3	Carbon_fiber	5.0e-4 μm	white
Layer 4	Carbon_fiber	1.0e-3 μm	white
Layer 5	Carbon_fiber	3.0e-3 μm	white
Layer 6	Carbon_fiber	5.0e-3 μm	white
Layer 7	Carbon_fiber	1.0e-2 μm	white
Layer 8	Carbon_fiber	3.0e-2 μm	white
Layer 9	Carbon_fiber	5.0e-2 μm	white
Layer 10	Carbon_fiber	2.0e-1 μm	white
Layer 11	Carbon_fiber	2.0e-1 μm	white
Layer 12	Carbon_fiber	5.0e-1 μm	white
Layer 13	Carbon_fiber	1.0 μm	white
Layer 14	Carbon_fiber	3.0 μm	white
Layer 15	Carbon_fiber	5.0 μm	white
Layer 16	Carbon_fiber	20.0 μm	white
Layer 17	Carbon_fiber	70. μm	white
Layer 18	Carbon_fiber	200. μm	white
Layer 19	Carbon_fiber	700. μm	white
Layer 20	Carbon_fiber	4000. μm	white

Visualisation

Format: Encapsulated PostScript (EPS)

Particle tracks: Display

Case C — Geometry: User defined

Shape: planar slab — Number of layers: 20

Layer number	Material	Thickness (unit)	Visualisation colour
Layer 1	Resin	2.0e-4 μm	white
Layer 2	Resin	3.0e-4 μm	white
Layer 3	Resin	5.0e-4 μm	white
Layer 4	Resin	1.0e-3 μm	white
Layer 5	Resin	3.0e-3 μm	white
Layer 6	Resin	5.0e-3 μm	white
Layer 7	Resin	1.0e-2 μm	white
Layer 8	Resin	3.0e-2 μm	white
Layer 9	Resin	5.0e-2 μm	white
Layer 10	Resin	2.0e-1 μm	white
Layer 11	T300	2.0e-1 μm	white
Layer 12	T300	5.0e-1 μm	white
Layer 13	T300	1.0 μm	white
Layer 14	T300	3.0 μm	white
Layer 15	T300	5.0 μm	white
Layer 16	T300	20.0 μm	white
Layer 17	T300	70. μm	white
Layer 18	T300	200. μm	white
Layer 19	T300	700. μm	white
Layer 20	T300	4000. μm	white

Visualisation

Format: Encapsulated PostScript (EPS)

Particle tracks: Display

Fluence Spectra for –Y, -X, and +X Environments (50%)

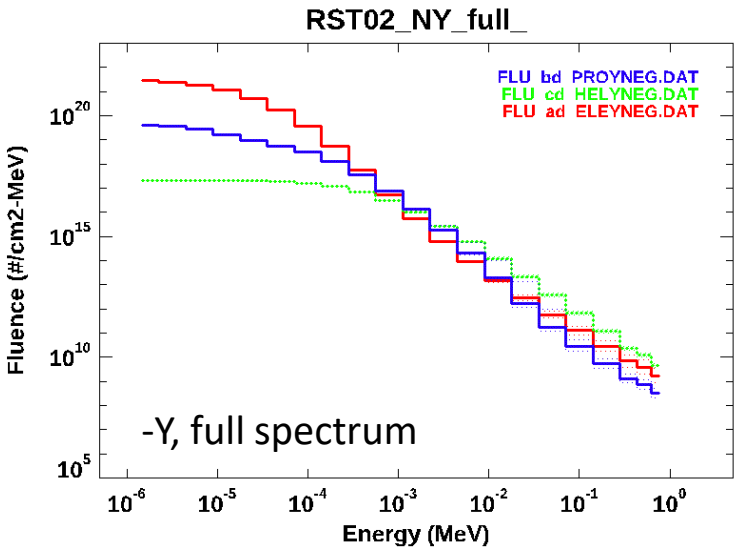

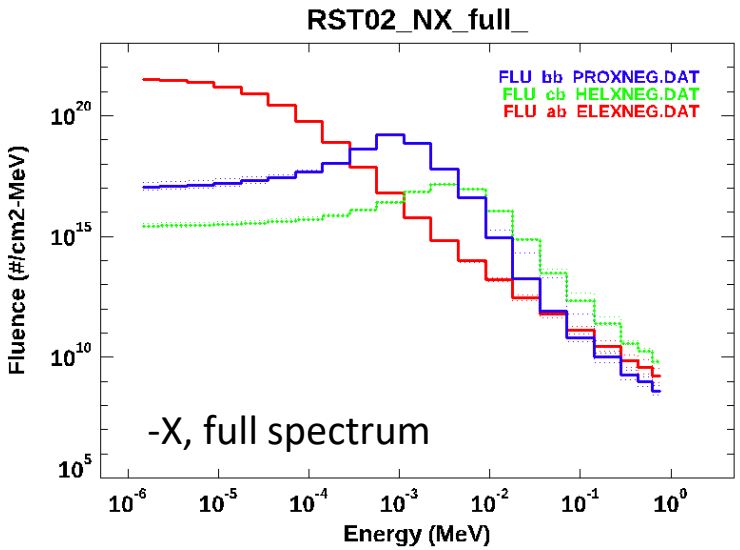

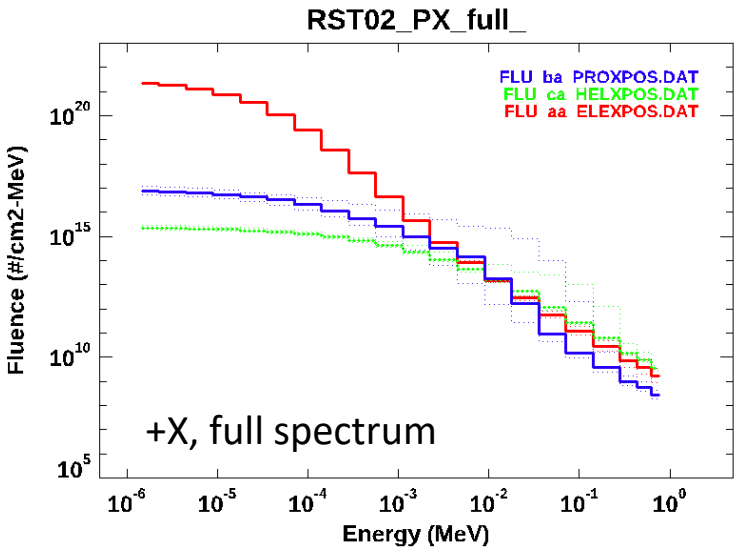

Dose-Depth Results for Case A (pure resin): -Y, -X, and +X environments

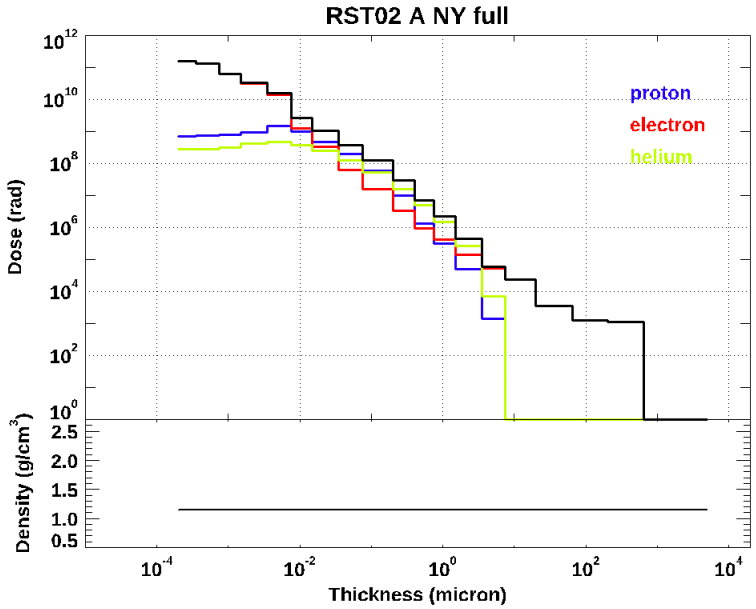

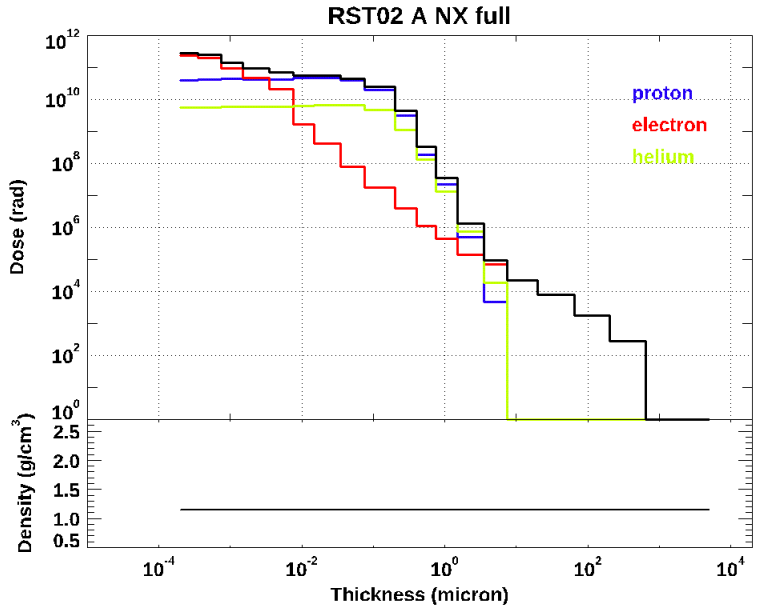

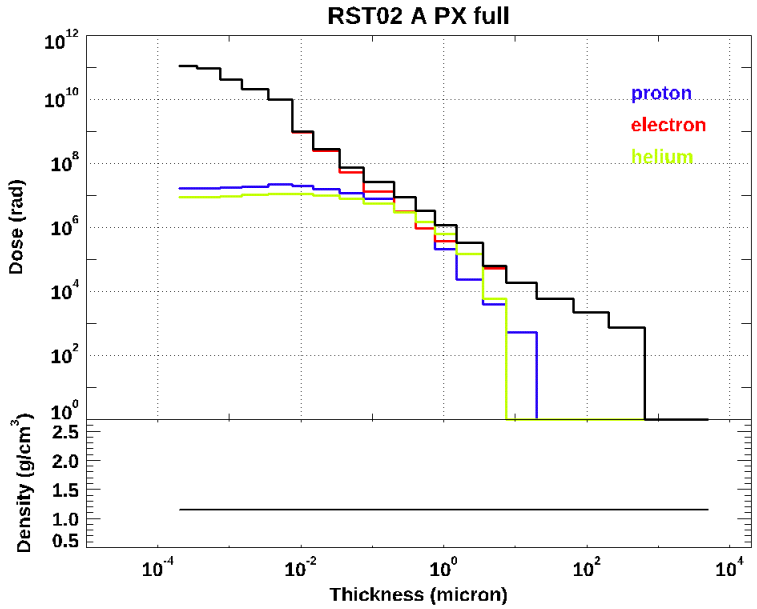

- All three environments give 109 to 1011 rad (1 Grad to 100 Grad) doses in the first 0.01 micron
- Sun facing surfaces (-X environment) has >0.1 Grad dose to depth of nearly 1 micron
- Electrons dominate surface dose for –Y, +X environments
- Protons dominate surface dose for –X environment

RST02_A_NX_full Case A, -X, full spectra

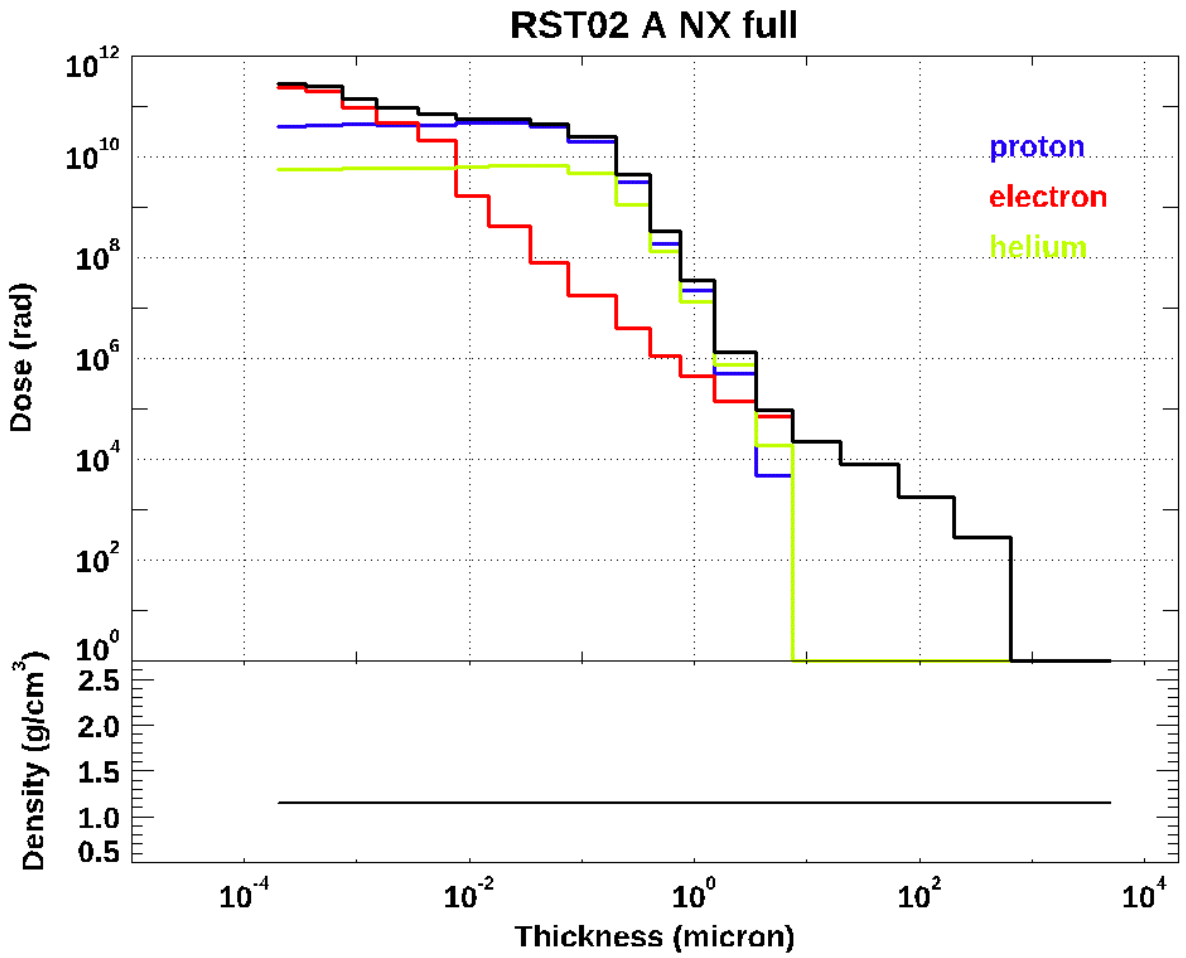

Layer Number	Layer Thickness (micron)	Cumulative Thickness (micron)	Density (g/cm3)	Dose Proton (rad)	Dose Electron (rad)	Dose Helium (rad)	Dose Total (rad)
1	2.000e-04	2.000e-04	1.140	4.059e+10	2.309e+11	5.674e+09	2.772e+11
2	3.000e-04	5.000e-04	1.140	4.196e+10	1.987e+11	5.696e+09	2.463e+11
3	5.000e-04	1.000e-03	1.140	4.358e+10	9.472e+10	5.817e+09	1.441e+11
4	1.000e-03	2.000e-03	1.140	4.330e+10	4.765e+10	5.902e+09	9.686e+10
5	3.000e-03	5.000e-03	1.140	4.188e+10	2.091e+10	6.107e+09	6.889e+10
6	5.000e-03	1.000e-02	1.140	4.651e+10	1.686e+09	6.453e+09	5.465e+10
7	1.000e-02	2.000e-02	1.140	4.826e+10	4.185e+08	6.762e+09	5.544e+10
8	3.000e-02	5.000e-02	1.140	3.912e+10	7.943e+07	6.505e+09	4.571e+10
9	5.000e-02	1.000e-01	1.140	2.007e+10	1.747e+07	4.695e+09	2.478e+10
10	2.000e-01	3.000e-01	1.140	3.229e+09	3.894e+06	1.137e+09	4.370e+09
11	2.000e-01	5.000e-01	1.140	1.936e+08	1.099e+06	1.313e+08	3.260e+08
12	5.000e-01	1.000e+00	1.140	2.246e+07	4.524e+05	1.332e+07	3.623e+07
13	1.000e+00	2.000e+00	1.140	4.890e+05	1.397e+05	7.416e+05	1.370e+06
14	3.000e+00	5.000e+00	1.140	4.850e+03	6.983e+04	1.832e+04	9.300e+04
15	5.000e+00	1.000e+01	1.140	0.000e+00	2.288e+04	0.000e+00	2.288e+04
16	2.000e+01	3.000e+01	1.140	0.000e+00	7.777e+03	0.000e+00	7.777e+03
17	7.000e+01	1.000e+02	1.140	0.000e+00	1.777e+03	0.000e+00	1.777e+03
18	2.000e+02	3.000e+02	1.140	0.000e+00	2.814e+02	0.000e+00	2.814e+02
19	7.000e+02	1.000e+03	1.140	0.000e+00	0.000e+00	0.000e+00	0.000e+00
20	4.000e+03	5.000e+03	1.140	0.000e+00	0.000e+00	0.000e+00	0.000e+00

RST02_B_NX_full Case B, -X full spectra

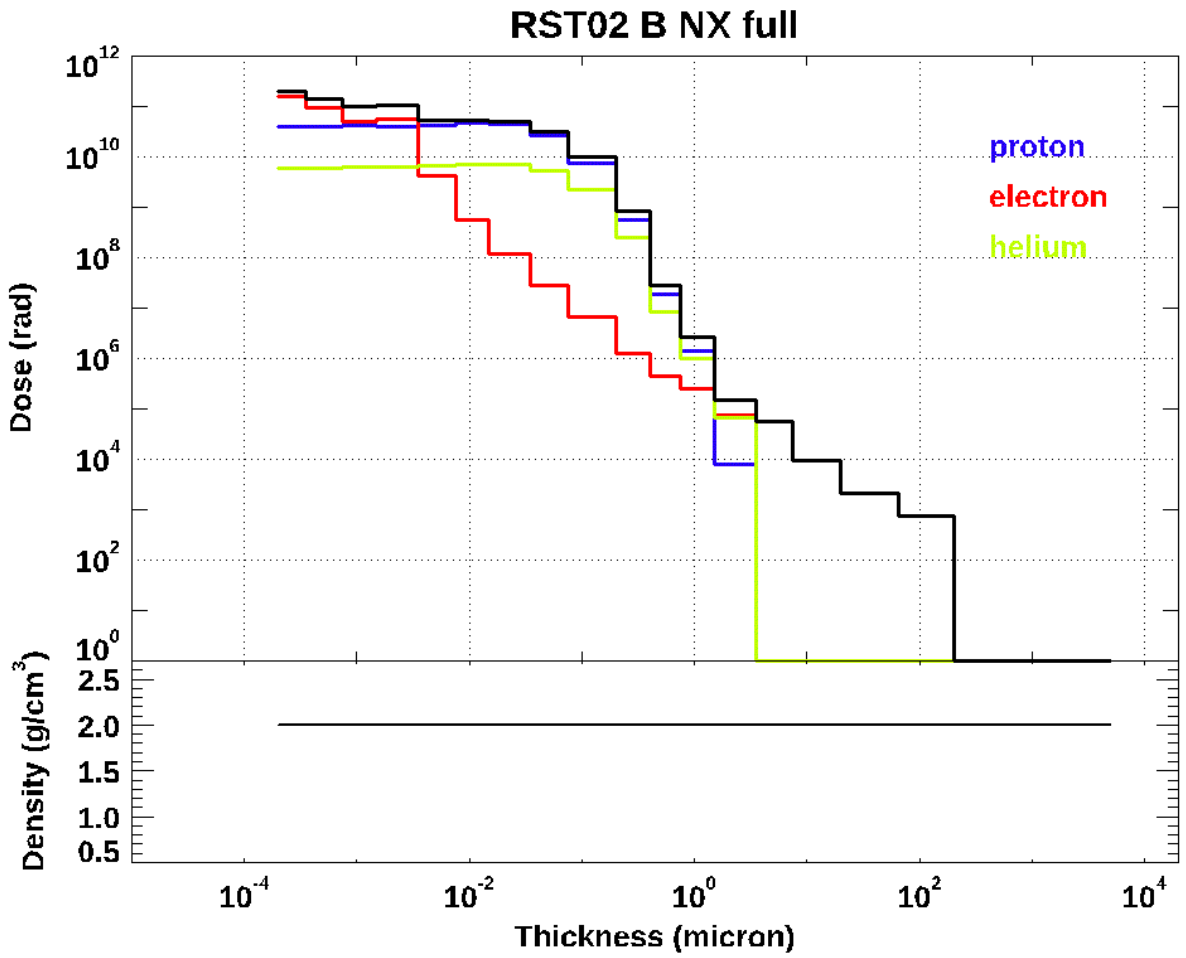

Layer Number	Layer Thickness (micron)	Cumulative Thickness (micron)	Density (g/cm3)	Dose Proton (rad)	Dose Electron (rad)	Dose Helium (rad)	Dose Total (rad)
1	2.000e-04	2.000e-04	2.000	3.974e+10	1.552e+11	6.079e+09	2.010e+11
2	3.000e-04	5.000e-04	2.000	4.071e+10	9.582e+10	6.103e+09	1.426e+11
3	5.000e-04	1.000e-03	2.000	4.138e+10	5.054e+10	6.185e+09	9.810e+10
4	1.000e-03	2.000e-03	2.000	3.950e+10	5.717e+10	6.299e+09	1.030e+11
5	3.000e-03	5.000e-03	2.000	4.223e+10	4.117e+09	6.603e+09	5.295e+10
6	5.000e-03	1.000e-02	2.000	4.694e+10	5.722e+08	7.044e+09	5.455e+10
7	1.000e-02	2.000e-02	2.000	4.400e+10	1.185e+08	7.101e+09	5.122e+10
8	3.000e-02	5.000e-02	2.000	2.646e+10	2.740e+07	5.452e+09	3.194e+10
9	5.000e-02	1.000e-01	2.000	7.502e+09	6.825e+06	2.296e+09	9.805e+09
10	2.000e-01	3.000e-01	2.000	5.780e+08	1.262e+06	2.451e+08	8.243e+08
11	2.000e-01	5.000e-01	2.000	1.925e+07	4.573e+05	8.345e+06	2.805e+07
12	5.000e-01	1.000e+00	2.000	1.417e+06	2.458e+05	9.797e+05	2.642e+06
13	1.000e+00	2.000e+00	2.000	7.836e+03	7.682e+04	6.725e+04	1.519e+05
14	3.000e+00	5.000e+00	2.000	0.000e+00	5.677e+04	0.000e+00	5.677e+04
15	5.000e+00	1.000e+01	2.000	0.000e+00	9.663e+03	0.000e+00	9.663e+03
16	2.000e+01	3.000e+01	2.000	0.000e+00	2.056e+03	0.000e+00	2.056e+03
17	7.000e+01	1.000e+02	2.000	0.000e+00	7.522e+02	0.000e+00	7.522e+02
18	2.000e+02	3.000e+02	2.000	0.000e+00	0.000e+00	0.000e+00	0.000e+00
19	7.000e+02	1.000e+03	2.000	0.000e+00	0.000e+00	0.000e+00	0.000e+00
20	4.000e+03	5.000e+03	2.000	0.000e+00	0.000e+00	0.000e+00	0.000e+00

RST02_C_NX_full Case C, -X, full spectra

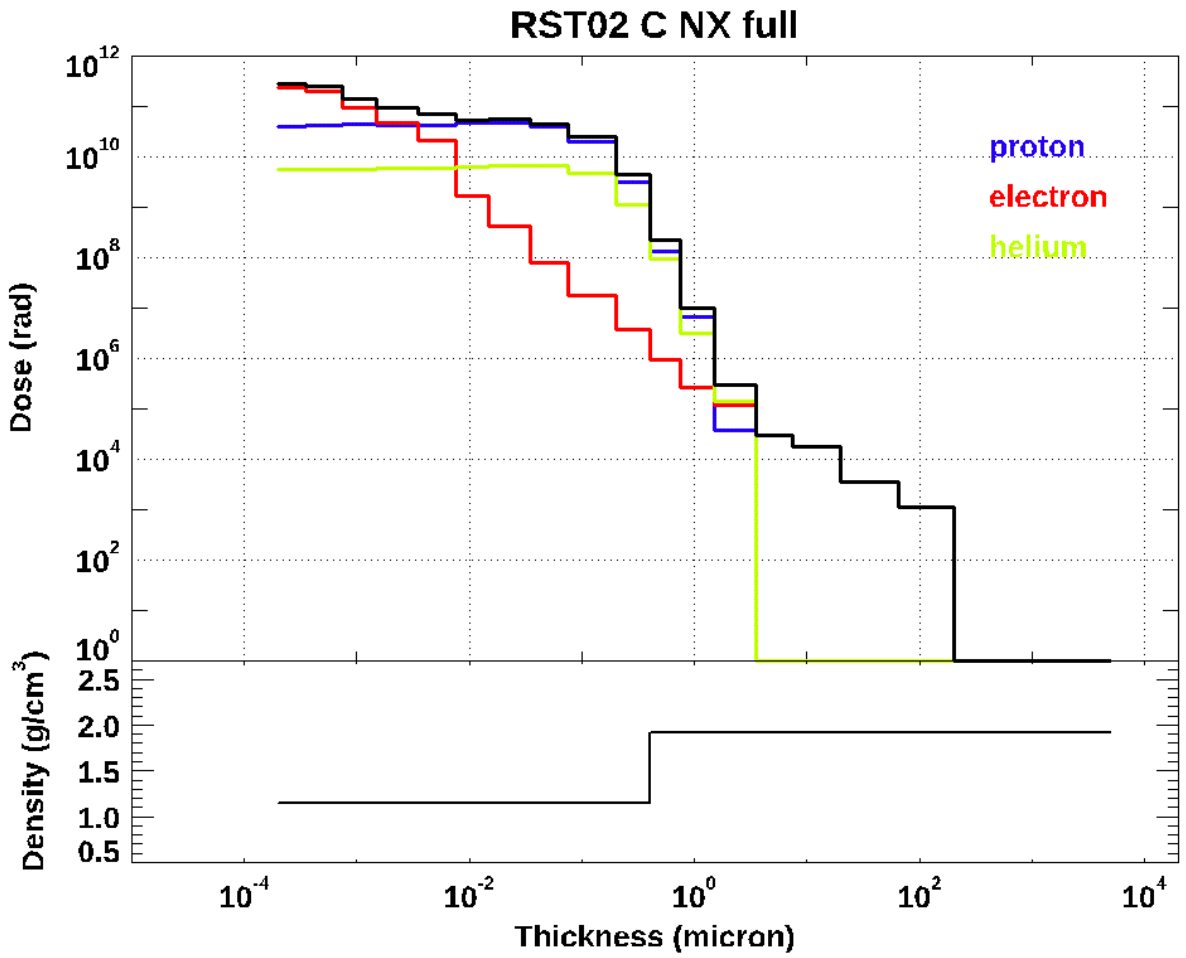

Layer Number	Layer Thickness (micron)	Cumulative Thickness (micron)	Density (g/cm3)	Dose Proton (rad)	Dose Electron (rad)	Dose Helium (rad)	Dose Total (rad)
1	2.000e-04	2.000e-04	1.140	4.061e+10	2.309e+11	5.662e+09	2.772e+11
2	3.000e-04	5.000e-04	1.140	4.193e+10	1.987e+11	5.711e+09	2.463e+11
3	5.000e-04	1.000e-03	1.140	4.354e+10	9.472e+10	5.785e+09	1.440e+11
4	1.000e-03	2.000e-03	1.140	4.339e+10	4.765e+10	5.892e+09	9.693e+10
5	3.000e-03	5.000e-03	1.140	4.188e+10	2.091e+10	6.100e+09	6.889e+10
6	5.000e-03	1.000e-02	1.140	4.650e+10	1.686e+09	6.450e+09	5.463e+10
7	1.000e-02	2.000e-02	1.140	4.824e+10	4.185e+08	6.763e+09	5.542e+10
8	3.000e-02	5.000e-02	1.140	3.912e+10	7.945e+07	6.507e+09	4.571e+10
9	5.000e-02	1.000e-01	1.140	2.008e+10	1.742e+07	4.697e+09	2.479e+10
10	2.000e-01	3.000e-01	1.140	3.229e+09	3.841e+06	1.136e+09	4.369e+09
11	2.000e-01	5.000e-01	1.914	1.331e+08	9.234e+05	9.182e+07	2.259e+08
12	5.000e-01	1.000e+00	1.914	6.874e+06	2.695e+05	3.131e+06	1.027e+07
13	1.000e+00	2.000e+00	1.914	3.760e+04	1.211e+05	1.454e+05	3.041e+05
14	3.000e+00	5.000e+00	1.914	0.000e+00	2.959e+04	0.000e+00	2.959e+04
15	5.000e+00	1.000e+01	1.914	0.000e+00	1.804e+04	0.000e+00	1.804e+04
16	2.000e+01	3.000e+01	1.914	0.000e+00	3.475e+03	0.000e+00	3.475e+03
17	7.000e+01	1.000e+02	1.914	0.000e+00	1.099e+03	0.000e+00	1.099e+03
18	2.000e+02	3.000e+02	1.914	0.000e+00	0.000e+00	0.000e+00	0.000e+00
19	7.000e+02	1.000e+03	1.914	0.000e+00	0.000e+00	0.000e+00	0.000e+00
20	4.000e+03	5.000e+03	1.914	0.000e+00	0.000e+00	0.000e+00	0.000e+00

Solar Wind vs Solar Particle Event Dose

- Genesis L1 solar wind environment, 24 August 2001 to 1 April 2004 (the time the Genesis capsule was open to the solar wind)
- Ion dose computed using TRIM code and converting ionization events into total ionizing dose
- Emission of Solar Proton (ESP) Model
- Source: *Minow et al., AIAA 2007-909, 45th AIAA Aerospace Sciences Meeting and Exhibit, Reno, NV, 8-11 Jan 2007.*

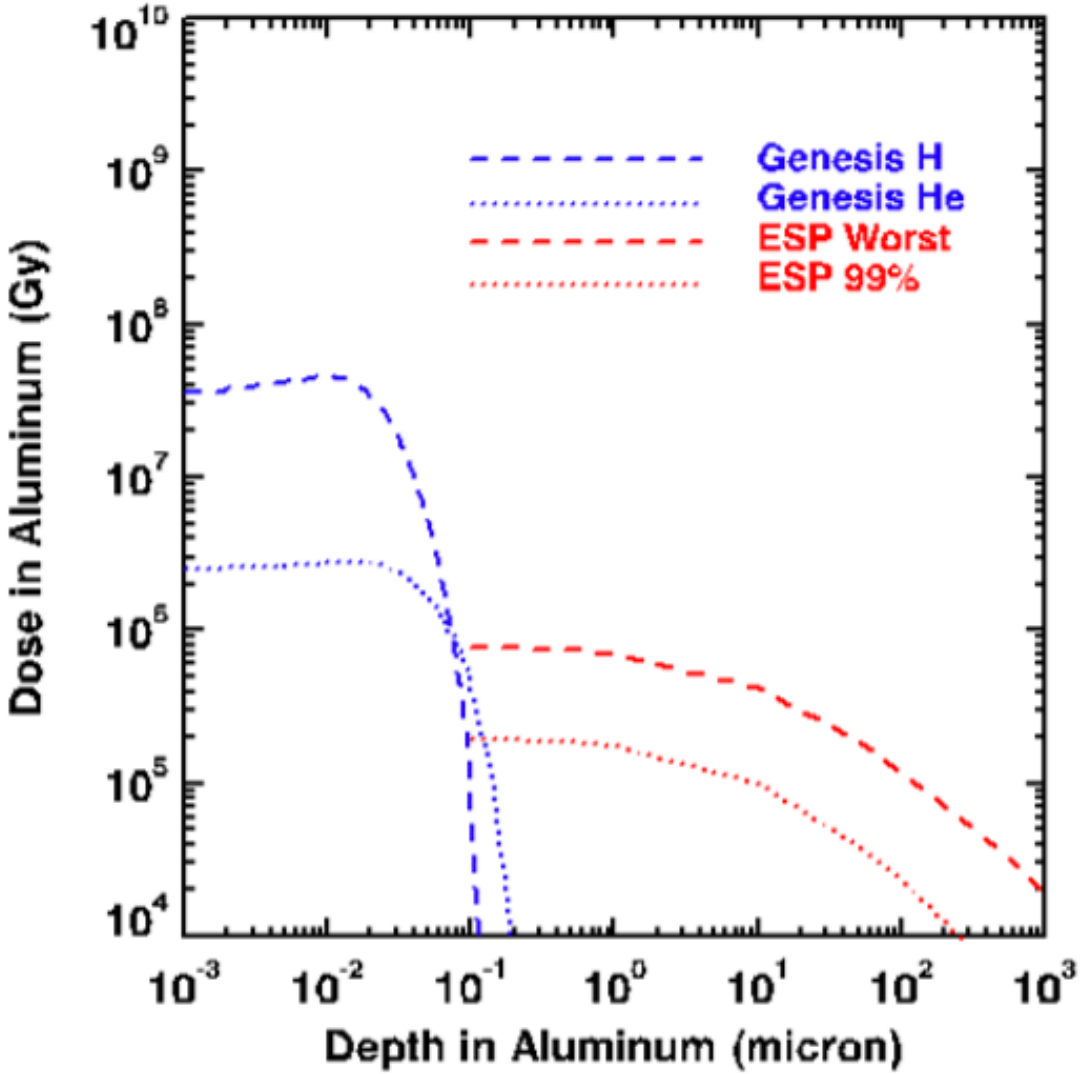

Discussion and Summary

- L2-CPE is a convenient tool for computing low energy charged particle fluence for missions in near Earth space that encounter the solar wind, magnetosheath, and magnetotail

- Graph and text output files provide users with options for examining model results and incorporating them into other analysis codes
  - Energy spectra can be rewritten into formats required for input to standard radiation transport codes to compute total ionizing dose, displacement damage to materials
  - Convolution of light ion energy spectra with energy dependent sputter yields are used to estimate sputter erosion of surface materials
  - Proton fluence are used for estimating H blistering of soft metals

- L2-CPE output easily ingested into radiation transport codes to compute radiation dose

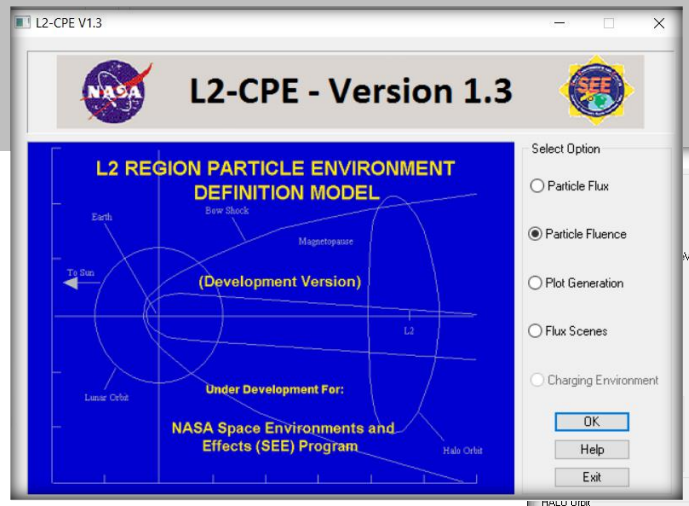

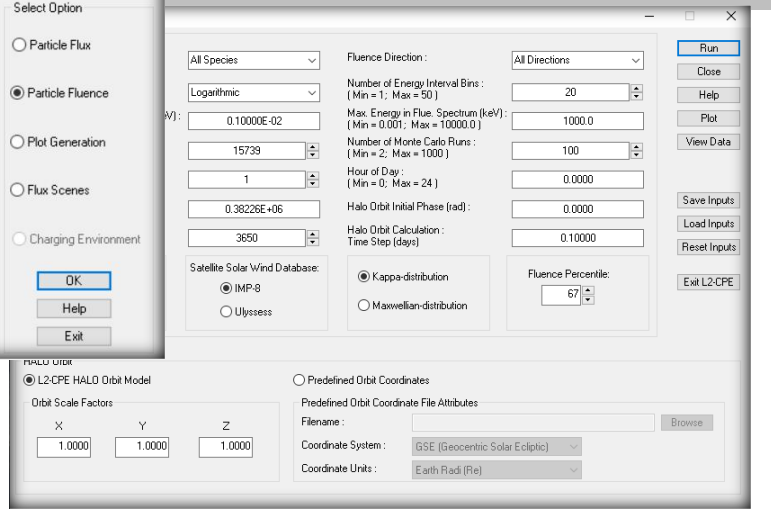

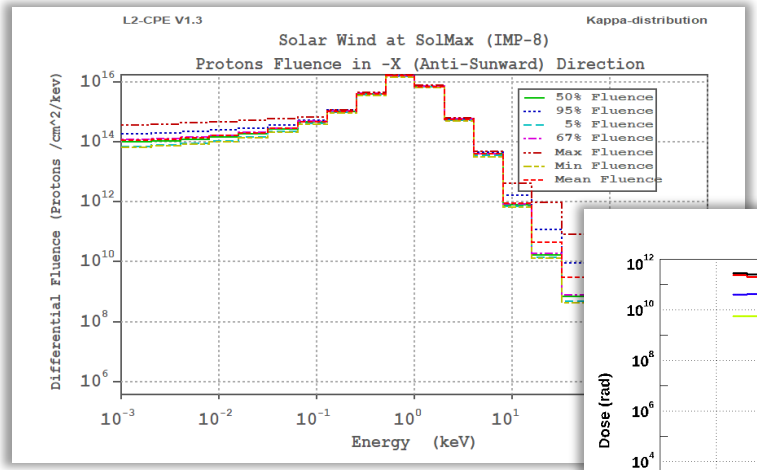

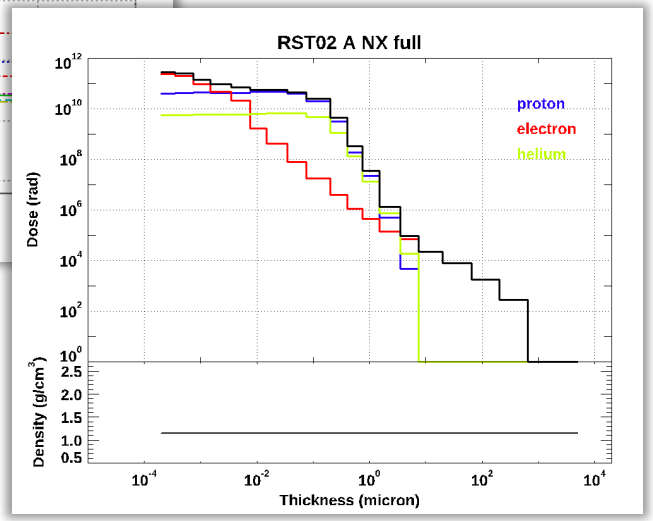

Questions?

joseph.minow@nasa.gov

Acronyms and Nomenclature

ACE	Advanced Composition Explorer (s/c)
AE8/AP8	Earth electron and proton radiation belt models
AE9/AP9	updated Earth electron and proton radiation belt models
APL	Applied Physics Laboratory (JHU)
ARIEL	Atmospheric Remote-sensing Infrared Exoplanet Large-survey (s/c)
ATHENA	Advanced Telescope for High-Energy Astrophysics (s/c)
AU	astronomical unit
CPI	Comprehensive Plasma Instrument (Geotail)
CREME96	Cosmic Ray Effects on Microelectronics 19960
DSCOVR	Deep Space Climate Observatory (s/c)
EPIC	Energetic Particles and Ion Composition (Geotail)
ESP	Emission of Solar Protons
eV	electron volt
GSE	geocentric solar ecliptic
GSFC	Goddard Space Flight Center
HabEx	Habitable Exoplanet Obseervatory (s/c)
HPA	Hot Plasma Analyzer (CPI, Geotail)
ICS	Ion Composition Subsystem (EPIC, Geotail)
IMAP	Interstellar Mapping and Acceleration Probe (s/c)
IRENE	International Radiation Environment Near Earth
ISEE-3	International Sun-Earth Explorer 3 (s/c)
JHU	Johns Hopkins University
JPL	The Jet Propulsion Laboratory
JWST	James Webb Space Telescope (s/c)
keV	thousand electron volts
Km	kilometer
LEFS	Low Energy Foil Spectrometer (Ulysses)
LEMS	Low Energy Magnetic Spectrometer (Ulysses)
LiteBIRD	Light satellite for the study of B-mode polarization and Inflation from cosmic background Radiation Detection (s/c)
LPF	Lisa Pathfinder (s/c)
LUVIOR	Large UV/Optical/IR Surveyor (s/c)
L2-CPE	L2 Charged Particle Environment
MeV	million electron volts
MIRI	Mid-Infrared Instrument (JWST)
MIT	Massachusetts Institute of Technology
MS	magnetosheath
MSFC	Marshall Space Flight Center
MULASSIS	Multilayered Shielding Simulation Software
NEO	Near Earth Object
NESC	NASA Engineering and Safety Center
NIRCam	Near-Infrared Camera (JWST)
NSSDC	National Space Science Data Center (GSFC)
OSIRIS-REX	Origins, Spectral Interpretation, Resource Identification, Security-Regolith Explorer (s/c)
OST	Origins Space Telescope (s/c)
PLATO	Planetary Transits and Oscillations (s/c)
PM	plasma mantle
PS	plasmasheet
Re	mean Earth radius (=6371 km)
RST	Roman Space Telescope (s/c)
SAPPHIRE	Solar Accumulated and Peak Proton and Heavy Ion Radiation Environment
s/c	spacecraft
SEY	secondary electron yield
STEREO	Solar Terrestrial Relations Observatory (s/c)
SOHO	Solar and Heliospheric Observatory (s/c)
SW	solar wind
SWFO-L1	Space Weather Follow On-L1 (s/c)
SWOOPS	Solar Wind Observations Over the Poles of the Sun (Ulysses)
SwRI	Southwest Research Institute
TRIM	Transport of Ions in Matter
TPF	Terrestrial Planet Finder (s/c)
Wind	s/c
WMAP	Wilkerson Microwave Anisotropy Probe